MADDEN–JULIAN OSCILLATION

Bridging Weather and Climate

BY CHIDONG ZHANG

As a prime example of intraseasonal variability, the Madden–Julian Oscillation affects—and is pivotal to predicting—both weather and climate.

The conceptual separation of weather and climate is deeply rooted in our daily experience, as Herbertson (1901) put it: "Climate is what on an average we may expect, weather is what actually we get."[1] Translated into a scientific language, weather is a state of the atmosphere at a particular instance and climate is a set of statistics of an ensemble of many different states (Lorenz 1975). The weather–climate separation had its scientific basis in numerical prediction. It has been perceived that weather predictability comes from initiation conditions, while climate predictability from boundary conditions (Charney and Shukla 1977). This distinction would cease to exist in the modern practice of "seamless prediction" for weather and climate using "unified prediction models" (Hurrell et al. 2009; Brown et al. 2012). In such models, all components of the Earth system are coupled to each other, the only boundary condition needed is at the top of the atmosphere, and the source of predictability comes from, in addition to initiation conditions, the "memory" of slowly varying subsystems (the ocean, soil moisture, land, and sea ice), quasiperiodic phenomena, and known external forcing (Lorenz 1975). Yet, the weather–climate separation has penetrated so deep in our thinking that their traditional definitions are still often used in scientific and official documents, leaving a gaping vacancy in between. This vacancy is occupied by intraseasonal (20–90 days) variability.

Intraseasonal variability is by no means merely red noise filling the gap between synoptic and seasonal variability. Intraseasonal phenomena are distinct from higher- and lower-frequency variability by their significant spectral peaks and coherent spatial patterns. The Madden–Julian oscillation (MJO; Madden and Julian 1971, 1972) is the best example. Its large-scale signals in the atmospheric circulation, deep convection, and other variables propagating eastward slowly (~5 m s^{-1}) from the Indian to Pacific Oceans are the dominant component of the tropical intraseasonal variability. They are so robust that they can be discerned from raw data without statistical manipulation (Zhang 2005).

The MJO plays a critical role in connecting or bridging weather and climate. This bridging role can

AFFILIATIONS: ZHANG—RSMAS, University of Miami, Miami, Florida
CORRESPONDING AUTHOR: Chidong Zhang, RSMAS/MPO, University of Miami, 4600 Rickenbacker Causeway, Miami, FL 33133
E-mail: czhang@rsmas.miami.edu

The abstract for this article can be found in this issue, following the table of contents.
DOI:10.1175/BAMS-D-12-00026.1

In final form 28 February 2013

[1] A more commonly known quotation, "Climate is what we expect, weather is what we get," is from Heinlein (1973).

be appreciated from different perspectives. The MJO affects many weather and climate phenomena. Its effects on weather depend on the state or phase of certain climate phenomena (e.g., ENSO), and their combined effects may lead to extreme weather events. Climate modes under the influence of the MJO in turn modulate weather in many parts of the world. The MJO is involved in scale interactions across a wide range of spectrum from the diurnal cycle to interannual variability (Moncrieff et al. 2012). Forecast of the Earth system to serve the society requires seamless prediction that covers daily, intraseasonal, seasonal, interannual, and longer variabilities (Dole 2008; Brunet et al. 2010; Shapiro et al. 2010; Chang et al. 2011). Improved MJO forecasting benefits prediction of tropical cyclones (Vitart 2009; Vitart et al. 2010), extratropical weather regimes (Marshall et al. 2010; Vitart and Molteni 2010), and ENSO (Shi et al. 2009); serves users from many sectors of the society (Gottschalck et al. 2010); and helps close the gap between traditional weather and short-term climate prediction (Waliser et al. 2006).

This article provides a brief summary of MJO effects on certain types of weather and climate events. The author hopes to convince its readers that weather and climate must be treated as a continuum by including the MJO and intraseasonal variability in general and reinforce the notion that the societal need for weather and climate prediction must be met with improved understanding and forecast of the MJO (Waliser et al. 2003a).

DETECTING MJO INFLUENCES ON WEATHER AND CLIMATE

When discussing possible effects of the MJO on a particular type of weather or climate events, we must be mindful that all MJO episodes do not cause those events and all those events are not related to the MJO. The issue is whether and how the MJO may modulate the chances of occurrence, strengths, or spatial patterns/distributions of those events, as illustrated by examples given in this article.

MJO influences on weather events are commonly described as how those events vary with its phases. MJO phases can be defined in terms of the timing and locations of its center of convection (maximum rainfall anomalies) and associated wind fields. Most commonly used MJO phases are based on the real-time multivariate MJO (RMM) index of Wheeler and Hendon (2004). The RMM index is derived from a combined EOF analysis of daily anomalies in upper- and lower-level zonal wind and outgoing longwave radiation (OLR). MJO phases are defined by the principle components of the first two leading EOFs, normalized by their standard deviation (Fig. SB1). Each day, represented by a dot on the phase diagram, belongs to a particular phase. The distance of the dot from the center measures the amplitude of the MJO on that day. Composites of rainfall or any other field for each phase illustrate the canonical behavior of the MJO. In the boreal winter composite (Fig. SB2), the convection center of the MJO, represented by the maximum of positive anomalies in rainfall, starts over the Indian Ocean in phases 1–3, passes through the Maritime Continent in phases 4 and 5 and into the western Pacific in phases 6 and 7, and may continue their circumnavigating journey into the western hemisphere in phases 8 and 1 and thus complete its full cycle. During boreal summer, the zonal movement of the MJO convection center is accompanied by an additional northward movement associated with the Asian summer monsoon (Lawrence and Webster 2002). When the amplitude is less than 1 (within the circle on the phase diagram), the MJO is considered very weak or not existing (no MJO) and can be assigned as phase 0.

MJO influences on climate may also depend on its phases. Some climate events are more likely to start, amplify, or change sign in certain MJO phases than others. Some other climate phenomena are related to activities of a group of MJO events over a period (e.g., a season), instead of phases of individual MJO events. There can be a time lag between the group MJO activities and the climate phenomena they affect.

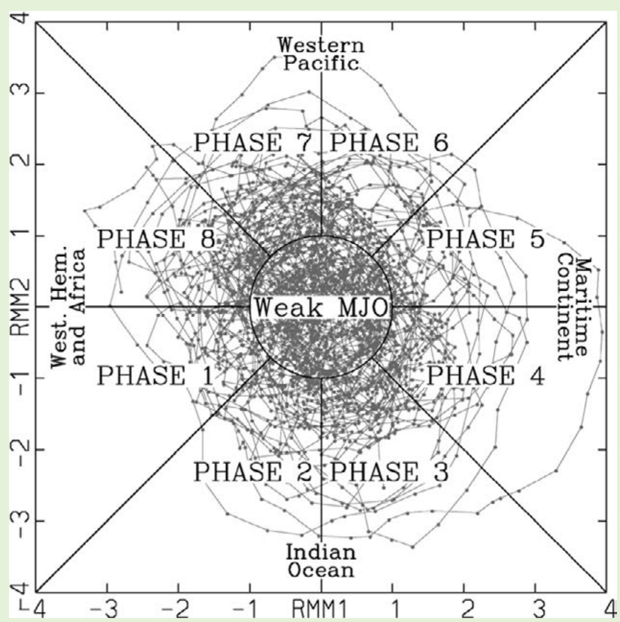

Fig. SB1 (above). Phase diagram of the RMM index. Each point represents a day. Eight phases and corresponding approximate locations of enhanced convective signals of the MJO are labeled. Points within the circle represent weak or no MJO (from Wheeler and Hendon 2004).

Fig. SB2 (right). Composites of intraseasonal (30–90 days) anomalies in TRMM precipitation (mm day^{-1}) during November–April of 1998–2012 based on the RMM index.

PRECIPITATION. The sidebar "Detecting MJO influences on weather and climate" (Fig. SB2) illustrates rainfall variability in the tropics associated with the MJO during boreal winter (November–April). MJO influences on precipitation are not limited to the tropics and this season. A global map of precipitation anomalies associated with MJO in austral winter is given in Fig. 1. Anomalies in precipitation change signs between MJO phases in many places of the world.

All monsoon systems undergo intraseasonal fluctuations (Lau and Waliser 2012). The MJO is a prominent source of the monsoon intraseasonal fluctuations. It affects the Asian summer monsoon mainly through, in addition to its eastward propagation, its northward propagation, which is unique in boreal summer. The onset of the South Asian monsoon is more likely to occur when MJO convection just starts over the Indian Ocean or in MJO phases 2 and 3 than in other phases. There are typically three or four major northward-propagating MJO events during a monsoon season, each inducing a local intraseasonal spike in rainfall. About 50%–80% of the total intraseasonal variance in the Asian summer monsoon rainfall is related to the MJO. On top of that, rainfall from synoptic monsoon lows and depressions enhanced by the MJO increases the chance of floods. Goswami (2012) and Hsu (2012) provided detailed descriptions of the role of the MJO in the Asian summer monsoon.

The MJO affects the Australian monsoon as its convection center propagates eastward, passing over the northern part of Australia (Wheeler et al. 2009). MJO accounts for more than 80% of onset dates of the Australian monsoon. Heavy rain (weekly rainfall in the top quintile of the December–February season) varies from 130 mm near the coast to 10 mm in central Australia. The probability of heavy rain at a given location depends on the longitudes of the MJO convection center. A detailed review on the role of the MJO in the Australia monsoon is given by Wheeler and McBride (2012).

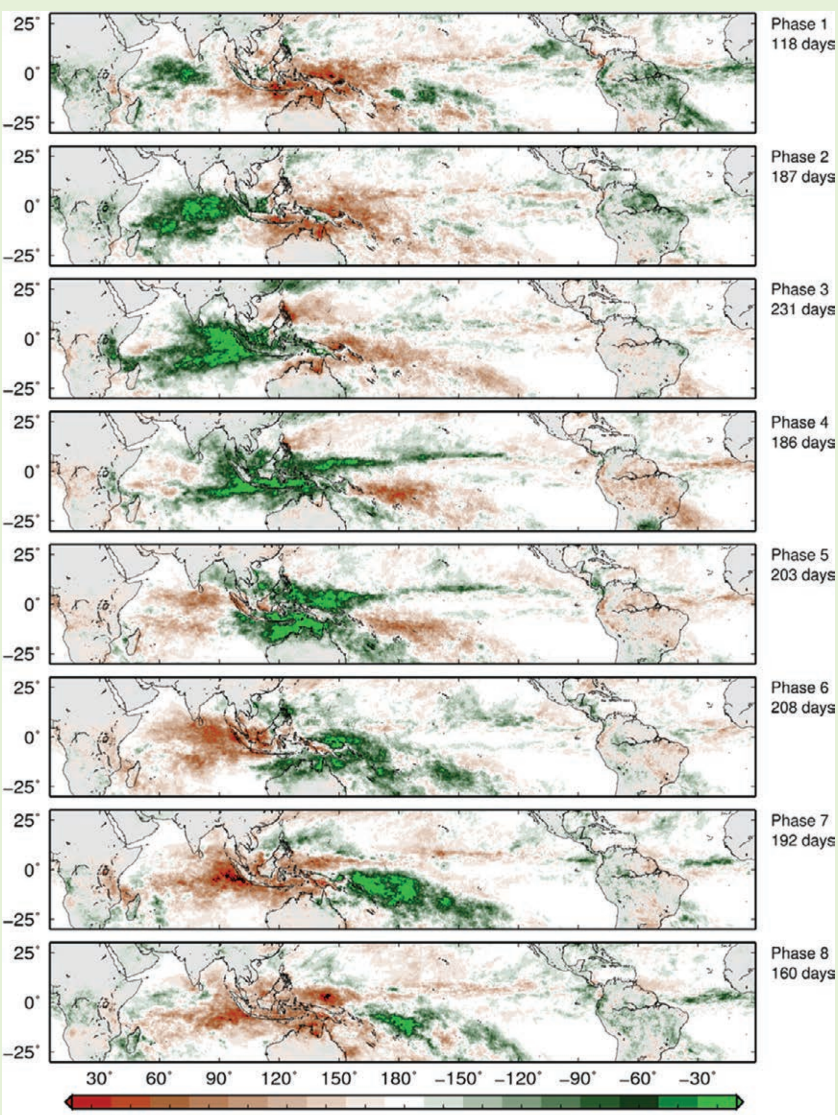

Large-scale perturbations that are excited by MJO convection and propagate into the Americas can induce intraseasonal fluctuations in rainfall of the American monsoons. In austral summer, rainfall over southern Brazil is heavier than normal (by up to 15–20 mm day^{-1}; 50%–75% of the mean) when MJO convection moves into the central Pacific, especially east of the date line, or when it starts over the Indian Ocean, but it is lighter than normal when the MJO convection center is near or immediately east of the Maritime Continent. In boreal summer, MJO convective activities along the ITCZ over the northeastern tropical

Pacific make it easier for the MJO to influence the North American monsoon. Its rainfall can differ as much as 25%–100% at individual stations between opposite phases of the MJO during July–September. The largest changes are along the Pacific coast, over southern Mexico and Central America, and on the Gulf coast of Mexico. Mo et al. (2012) provided a detailed summary of the role of the MJO in the pan-American monsoons.

Over West Africa, intraseasonal variability accounts about 30% of the total monsoon rainfall. One-third of the intraseasonal variability is related to the MJO or the African MJO mode (Janicot et al. 2011). At certain locations rainfall fluctuates by a factor of 2 between MJO phases. Near Lake Chad, about 50% of the amplitude of intraseasonal convective anomalies is related to the MJO (Alaka and Maloney 2012). From there, rainfall anomalies move westward to the rest of West Africa, presumably related to the Rossby waves generated by MJO convection over the Indian Ocean (Matthews 2004). As these convective systems move westward, some of them become part of African easterly waves. These African easterly waves are enhanced when the MJO convection center is over the Indian Ocean and suppressed when it is over the Maritime Continent and western Pacific (Ventrice et al. 2011). Janicot et al. (2011) and Barlow (2012) described in detail the MJO influences on the West African monsoon.

MJO also influences precipitation outside the monsoon regions and monsoon rainy seasons. Examples can be found in the Middle East and Southwest Asia (Barlow et al. 2005; Barlow 2012), Southeast and East Asia (Jeong et al. 2008; Zhang et al.2009; He et al. 2011; Jia et at. 2011), equatorial Africa (Pohl and Camberlin 2006a, b; Laing et al. 2011), Brazil (Carvalho et al. 2004; Souza and Ambrizzi 2006), Chile (Barrett et al. 2012), and North America (Bond and Vecchi 2003; Becker et al. 2011).

MJO influences on precipitation extend to extreme rainfall, defined as precipitation breaking the records or within a given top percentile. On a global scale, extreme rainfall events during active MJO periods (phases 1–8) are about 40% higher than in its quiescent periods (phase 0) (Jones et al. 2004). The MJO might have been one of the factors for the heavy snowfalls in the Tokyo metropolitan area on 3 February 2008 (Yamakawa and Suppiah 2009). The record-breaking snow events in the eastern United States in December 2009 and February 2010 was attributed to the MJO with its unusual active convection over the central Pacific during an El Niño year on top of the negative phase of the North Atlantic Oscillation (Moon et al. 2012). Over the highland region of east

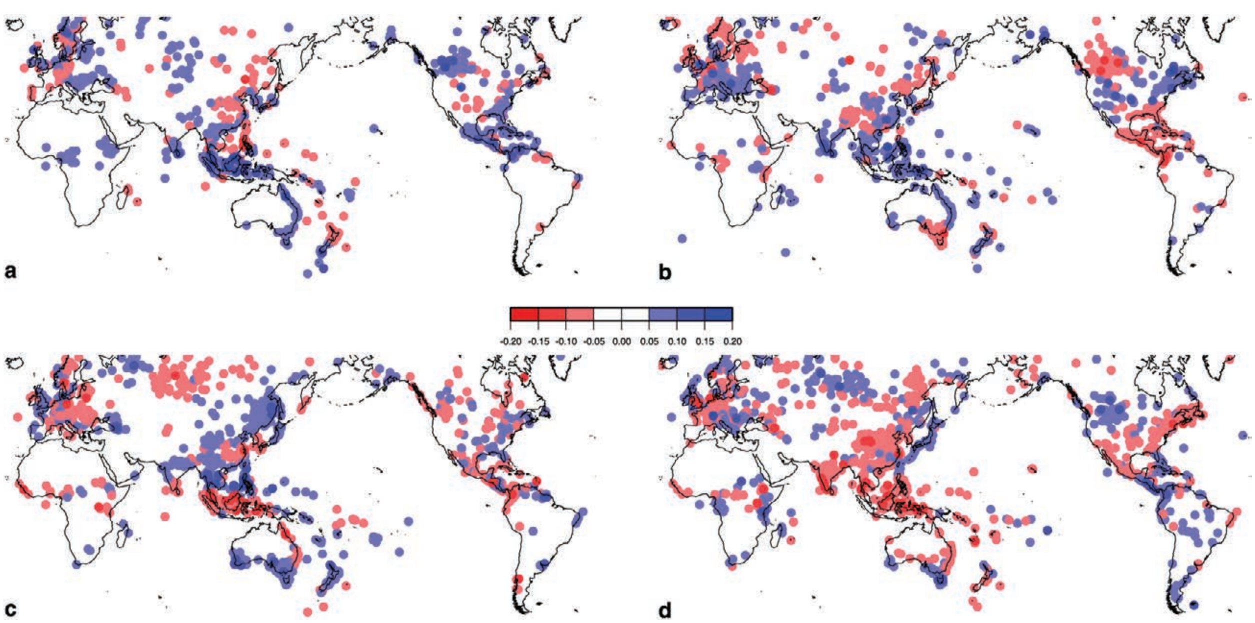

Fig. 1. Rainfall anomalies measured by surface rain gauges during MJO phases (a) 2, (b) 4, (c) 6, and (d) 8 for austral winter. Anomalies are expressed as maximum vertical distance between the unconditional cumulative distribution function (CDF) and the corresponding conditional CDF for a particular MJO phase (vertical differences are measured at the point of maximum divergence in dimensionless units of "percent change in probability"). Positive (negative) distances indicate evidence of enhanced (suppressed) rainfall during the respective phase (from Donald et al. 2006).

equatorial Africa, 62% of extreme rainfall events in March–May occur when MJO convection over the Indian Ocean is active, while 72% of extreme rainfall near the coastal region occurs when MJO convection is suppressed over the Indian Ocean and Maritime Continent. There, negative anomalies during weak MJO years often follow the peaks of ENSO warm events (Pohl and Camberlin 2006b). In the subtropical, semiarid north-central coastal area of Chile (30°S), about 80% of the strong precipitation events (normally 3–5 per year) during the fall and winter of rainy years are related to enhanced MJO convection in the central equatorial Pacific (Juliá et al. 2012).

Extreme rainfall (exceeding 90th percentile of frequency distribution in intensity and spatial coverage) in boreal winter occurs twice more frequently over the contiguous United States when the MJO is active (phases 1–8) than inactive (phase 0) and most frequently when the MJO convection center is over the Indian Ocean (Jones and Carvalho 2012). Such MJO influences are stronger during ENSO warm than cold events. Forecast skill for the winter extreme precipitation is higher when MJO convection over the Indian–western Pacific Oceans are suppressed (Jones et al. 2011a,b).

The MJO affects precipitation in remote areas by modifying the strength of meridional overturning circulations (Zhang et al. 2009; He et al. 2011) and moisture transport (Jeong et al. 2008; Jia et al. 2011), exciting Rossby wave trains that emanate from the tropics into the extratropics (Grimm and Silva Dias 1995), and forcing zonally propagating equatorial Rossby and Kelvin waves (Matthews 2004; Janicot et al. 2009). A phenomenon known as the "atmospheric river" acts as a conveyer belt to transport moisture from the tropical central Pacific to the West Coast of the United States, where it may cause torrential rain and floods (Dettinger 2011). MJO may enhance rainfall along the West Coast of the United States through strengthening the atmospheric river (Ralph et al. 2011). As a result, total snow accumulation in the Sierra Nevada significantly increases (reduces) when MJO convection is active over the eastern Indian Ocean (Western Hemisphere); the corresponding magnitude of daily anomalies is about half the daily mean in the cold season (Guan et al. 2012).

TORNADOES. Violent tornado outbreak days, with six or more tornadoes on the (Enhanced) Fujita [(E)F] scale of at least (E)F2 magnitude reported within a 24-h period, tend to occur in spring over the contiguous United States. Thompson and Roundy (2013) documented that violent tornado outbreak days during March, April, and May are more than twice as frequent during MJO phase 2 as during other phases, including phase 0. Atmospheric conditions favorable for tornado formation can be provided by combined intraseasonal and seasonal anomalous patterns in upper-tropospheric troughs and upper- and lower-tropospheric winds.

TROPICAL CYCLONES. Favorable large-scale conditions for genesis, intensification, and longevity of tropical cyclones (TCs) can be altered by the MJO. Figure 2 shows TC tracks in different MJO phases and composites of precipitation anomalies of the MJO. The density of the tracks indicates total TC days or the TC occurrence frequency when normalized by the total days of each MJO phase. This figure summarizes the known MJO modulation of TCs that has been documented by many studies—some of which are mentioned below. It shows an obvious eastward shift of the most dense TC tracks along with the positive precipitation anomalies of the MJO from the Indian Ocean to the eastern Pacific.

Over the southern Indian Ocean, TCs are more frequent in MJO phases 2 and 3 than in phases 8 and 1. The number of TCs there tend to increase by twofold (Liebmann et al. 1994) or more precisely by a factor of 2.6 (Bessafi and Wheeler 2006), from periods of negative convective anomalies (or low-level easterly anomalies) of the MJO over the Indian Ocean to positive convective anomalies (or westerly anomalies). Between phases 2 and 3 and phases 4 and 5, heavy TC genesis locations shift eastward with the MJO convection center across the Indian Ocean (Ho et al. 2006). TCs occur most frequently in MJO phases 4 and 5 and least frequently in phases 8 and 1 over the northern Indian Ocean and also near the northwestern coast of Australia, with a difference of 4 to 1 (Hall et al. 2001).

Over the tropical southwestern Pacific, TCs appear most frequently in MJO phases 6 and 7 and least frequently in phases 4 and 5. Over the northwestern Pacific, TCs are most frequent in phases 6 and 7 and least frequent in phases 2 and 3. The MJO modulation of TCs over the Indian and western Pacific Oceans sometimes leads to twin tropical cyclones straddling at the equator (Keen 1982; Ferreira et al. 1996).

Over the tropical eastern Pacific, there are more TCs (hurricanes) in MJO phases 8 to 3 than in phases 4 and 5. TCs vary coherently with the low-level zonal wind anomalies of the MJO and there are over four times more hurricane-strength storms during westerly phases of the MJO than its easterly phases

(Maloney and Hartmann 2000a). Global models with sufficiently high grid spacing well capture this MJO–TC connection (Jiang et al. 2012).

The MJO can also considerably influence hurricanes in the Gulf of Mexico, Caribbean Sea, and tropical Atlantic (Mo 2000). More hurricanes tend to occur in MJO phases 2 and 3 than in phases 6 and 7. Differences in major hurricane numbers and hurricane days in the main development region (7.5°–22.5°N, 20°–75°W) are a factor of 3 (Klotzbach 2010). Hurricane genesis in these regions is four times more likely to occur in local low-level westerly wind phases of the MJO than in its easterly phases, and strong hurricanes (categories 3–5) have an even greater preference (fivefold) to occur during local westerly phases of the MJO (Maloney and Hartmann 2000b). Numerical prediction skill of Atlantic hurricanes sensitively depends on MJO phases and strength at model initiation time (Belanger et al. 2010).

Globally, more TCs tend to occur near the eastern edge and to the poleward side of the local low-level westerly wind anomalies of the MJO and within the eastern and equatorward portion of its cyclonic vortex gyres (Frank and Roundy 2006). Possible mechanisms for the MJO influences on TCs include reduced vertical wind shear, enhanced low-level convergence, cyclonic relative vorticity, deep convection, midlevel moisture, small eddies, and synoptic disturbances serving as embryos for TCs (Liebmann et al. 1994; Mo 2000;

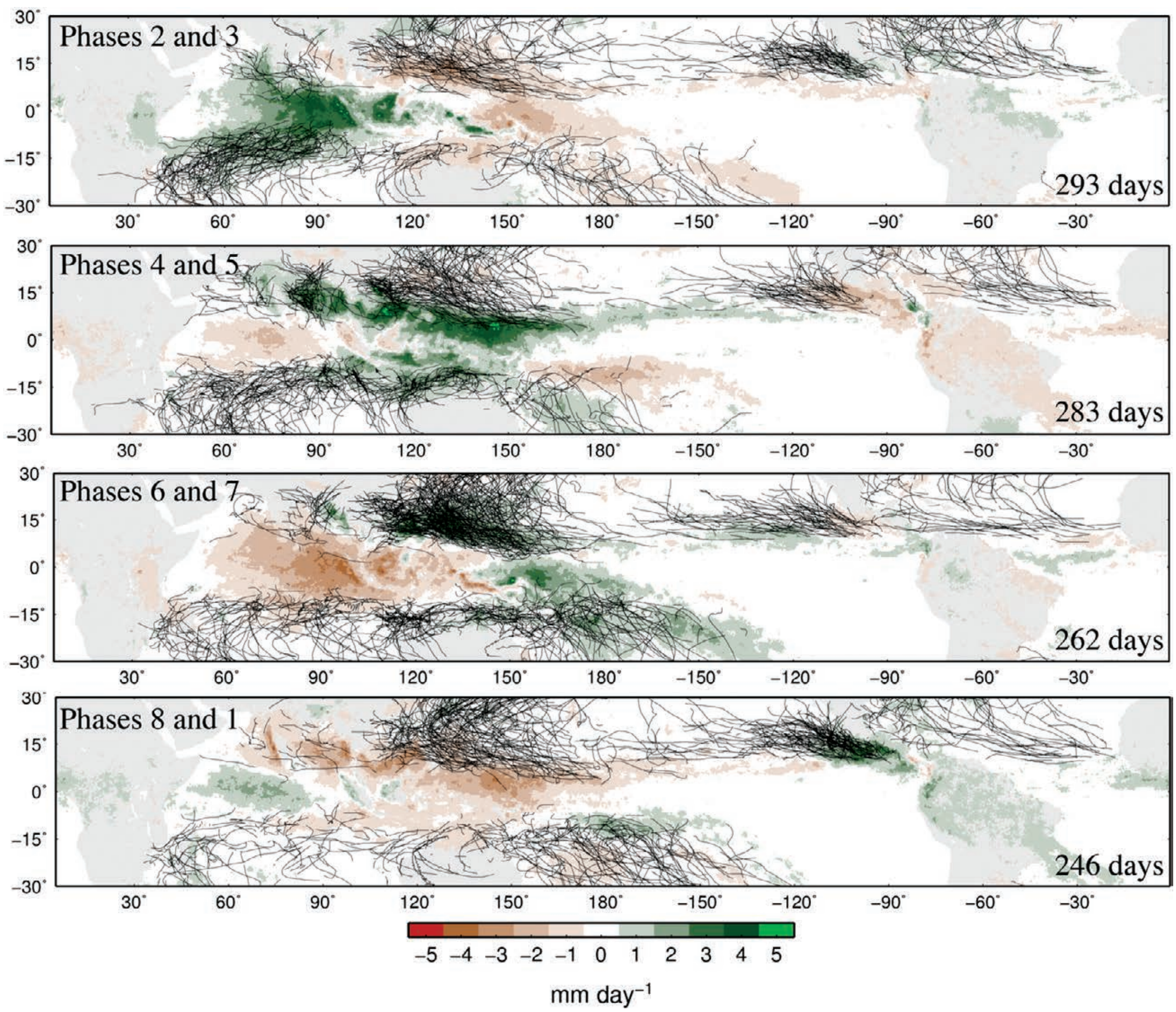

Fig. 2. TC tracks (1975–2011) and precipitation anomalies (1998–2011) in MJO phases 2 and 3, 4 and 5, 6 and 7, and 8 and 1 when the amplitude of the RMM index is greater than one. The total number of days of TCs in each phase group is listed. The TC tracks are from the International Best Track Archive for Climate Stewardship (IBTrACS) v03r04. Precipitation data are from Tropical Rainfall Measuring Mission (TRMM) 3B43 v7.

Maloney and Hartmann 2001; Maloney and Shaman 2008; Camargo et al. 2009).

Based on the observed modulation of TCs by the MJO, statistical models for predicting TC genesis or occurrence with lead times beyond one week have been developed (Leroy and Wheeler 2008; Slade and Maloney 2013). Dynamical models that can reproduce the observed relationship between the MJO and TCs attain skills of predicting their landfall (Vitart 2009). Their skill in predicting TCs up to 20 days has been attributed to their skill in predicting the MJO (Vitart et al. 2010).

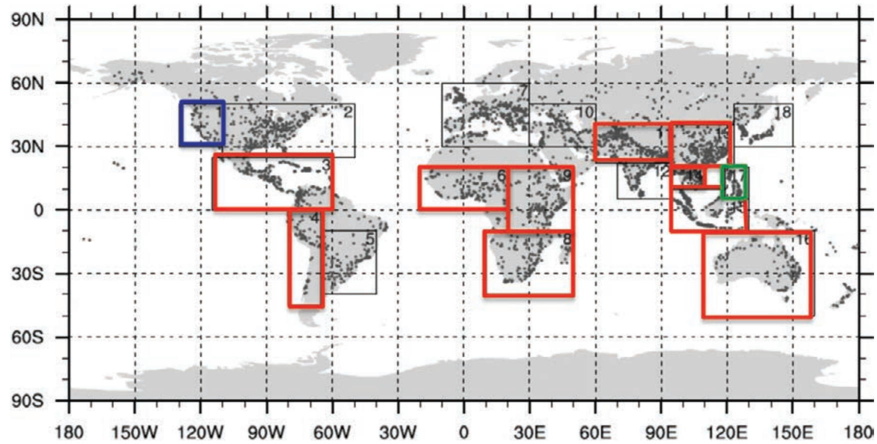

Fig. 3. Locations of large floods during 1985–2010 based on the Dartmouth Flood Observatory Global Archive of Large Flood Events at University of Colorado (http://floodobservatory.colorado.edu/Archives/index.html). Red boxes mark regions where probability of total flood days and/or events are significantly affected by the MJO. Blue and green boxes are examples shown in Figs. 4 and 5, respectively.

FLOOD. Observational studies have suggested that the MJO might have had influences on certain major flood events. Examples include a series of severe floods during the summer of 1998 in eastern China (Zhu et al. 2003), the Afghanistan flood of April 2002 (Barlow et al. 2005), the extreme 2006–07 flood in the southern peninsula of Malaysia (Tangang et al. 2008), and the largest floods on record at Jakarta in 2002, 2007, and 2008 (Aldrian 2008). While relating individual flood events to individual MJO events must face large uncertainties, MJO influences on flood occurrence probability can be quantified with statistical significance. An analysis of a global flood data (see http://floodobservatory.colorado.edu/Archives/index.html) suggested possible effects of the MJO on global "large flood events," which are defined as extreme flood events with damages that have been reported with intervals of a decade or longer. The locations of such large flood events are shown in Fig. 3. Several flood regions are defined, somewhat arbitrarily, based on known flood vulnerability (e.g., the Philippines) or geographic location (e.g., Australia). In a given region, flood probability is measured as the total number of flood days and flood events,[2] normalized by the total number of days in a given MJO phase or calendar month.

Over the West Coast of North America (blue box in Fig. 3), for example, there is a strong seasonal cycle in large floods, with many more flood days in December and January than in June and July (Fig. 4a). Most December and January floods occur when there are MJO events. While early winter (November–December) floods in the northwest United States tend to occur when MJO convection is active over the Indian Ocean (Bond and Vecchi 2003), large flood events are most likely to start in MJO phase 6 when its convection center is located over the western Pacific and least likely in phase 1 (Fig. 4b) when positive precipitation anomalies of the MJO are generally in the Western Hemisphere (Fig. SB2). Differences between these two phases and between them and phase 0 (no MJO) are significant at the 95% confidence level.

Another example is the Philippines (green box in Fig. 3), which is located on the pathway of MJO propagation. There, the seasonality of large flood is marked by a dip in April (Fig. 5a). Both total flood days (Fig. 5b) and flood events (Fig. 5c) are substantially higher in phases 6 and 7 than in phases 2 and 3, and both are significantly different from those in phase 0 (no MJO). The MJO modifies the occurrence probability of large flood days and/or events also in many other regions (red boxes in Fig. 3).

FIRE. Possible MJO effects on fire (biomass burning due both to wildfire and manmade fire in agriculture practice) come obviously from its modulation on rainfall that may help prevent, delay, or terminate fire. An example is the influence of the MJO on fire over the Maritime Continent, where biomass burning is part of the land management practice (Reid et al. 2012). During the dry and burning season (June–November), fire maximum (minimum) occurs during

[2] One flood event consists of all consecutive flood days.

local dry (rainy) phases (5–8 versus 1–4) of the MJO, as expected. The ratio of fire accounts between these phases can be as high as 10 (Fig. 6). The strongest MJO effects tend to occur in regions where convective rainfall is enhanced by orography (e.g., Sumatra, western Borneo). Similar results were obtained during the wet season (December–May) with two exceptions. Fire activity is more delayed after the rainy phases of the MJO because it takes longer for the burning materials to dry. Stronger MJO rainfall leads to much lower fire minimum than during dry seasons, effectively doubling the relative differences between fire maximum and minimum.

Globally, the MJO affects fire in many regions. A similar analysis method as for flood revealed that carbon fire emission (Mu et al. 2011) in certain parts of the world fluctuates substantially with MJO phases (Fig. 7). For example, over northwestern Canada and Alaska, fire is most likely to occur in MJO phase 1 and is least likely in phase 4. In northeastern China and adjacent Siberia, fire chances are also the lowest in MJO phase 4 but the highest in phase 7. MJO effects on fire in these high-latitude regions must be explained in terms of tropical–extratropical teleconnections.

LIGHTNING AND GLOBAL ELECTROMAGNETIC FIELD. Over the eastern tropical Indian Ocean, the maximum flash rate occurs slightly after OLR anomalies of the MJO reach maximum, and

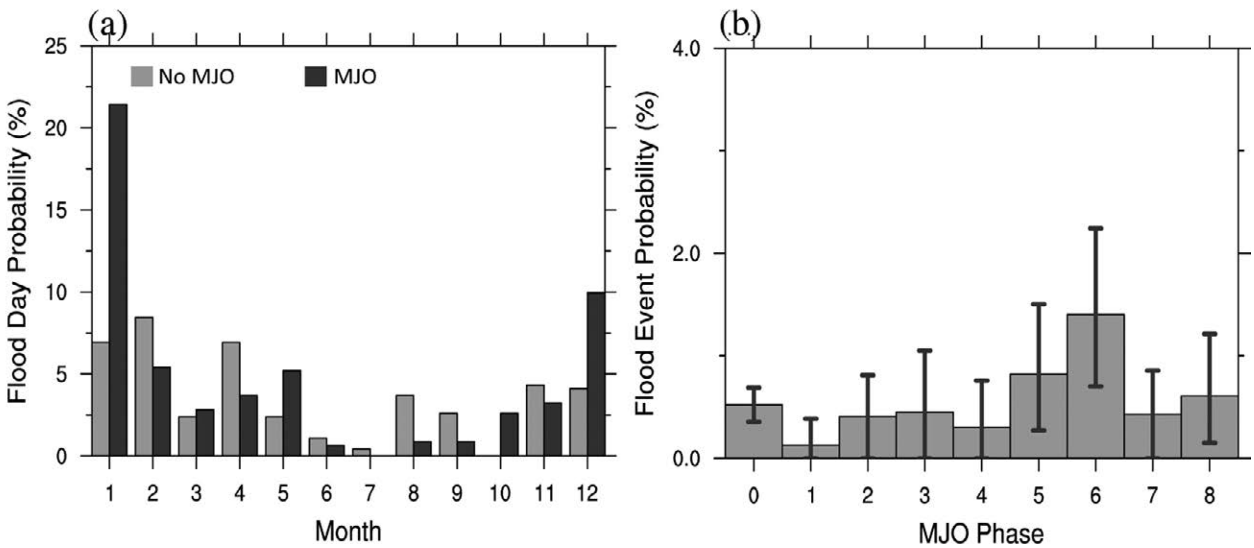

Fig. 4. MJO influences of large floods of the West Coast of North America (blue box in Fig. 3). (a) Monthly probability of total flood days during MJO episodes (black bars) and when there is no MJO (gray). (b) Probability of flood events in each MJO phase (total number of flood events starting in each phase divided by the total number of days in that phase). Vertical error bars denote ranges of the 95% confidence level.

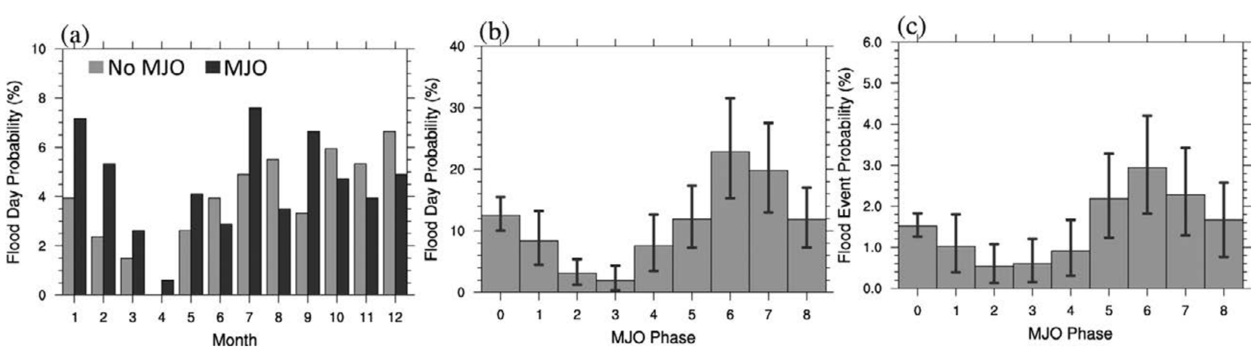

Fig. 5. MJO influences of large floods of the Philippines (green box in Fig. 3). (a) Monthly probability of total flood days during MJO episodes (black bars) and when there is no MJO (gray). (b) Probability of total flood days in each MJO phase (total number of flood days in each phase divided by the total number of days in that phase). (c) Probability of flood events as functions of MJO phases. Vertical error bars denote ranges of the 95% confidence level.

the minimum flash rate (about 18% lower than the maximum) slightly after OLR anomalies are minimum (Morita et al. 2006). For the same amount of rain, the flash rate increases when MJO convection is suppressed and rain systems tend to show more continental characteristics with isolated, very deep (>10 km) convective cells but decreases when MJO convection becomes active and rain systems tend to show more oceanic characteristics with wide-spread convection and moderate depth (~7 km). Over large islands of the Maritime Continent (e.g., Sumatra, Kalimantan), lightning frequency tends to reach its maximum (up to 50% of the climatological means) immediately prior to a local convectively active phase of the MJO and reach its minimum during and immediately after an inactive phase (Kodama et al. 2006; Virts et al. 2011). Such fluctuations in lightning activity through the convective life cycle of the MJO are consistent to the substantial amount of "vertically intense" convection observed in the suppressed period of the MJO and a lack of it in the active period over the ocean (Demott and Rutledge 1998a,b) and land (Shibagaki et al. 2006).

Cloud-to-ground lightning strikes can be an ignition mechanism for wildfire under relatively dry conditions, such as summer across vast sections of the western United States (Pyne et al. 1996). There is a strong connection between the MJO and summertime lightning activity across the United States (Fig. 8). Lightning activity tends to emanate northward from the desert southwest into the northern Rocky Mountains through MJO phases 6–8. After that, it quickly spreads eastward to the Great Lakes area and the east coast in phase 1. In addition, lightning frequency increases over 60% across the U.S. Southeast as the MJO convection center moves over the Maritime Continent (phase 6). It is argued that the MJO provides favorable conditions for the northward propagation of widespread lightning activity through the amplification of the upper-level ridge over the western United States and the development of midtropospheric instability (Abatzoglou and Brown 2009).

The Schumann resonances (SRs) are electromagnetic waves of zonal wavenumber one trapped in the natural cavity between Earth and the ionosphere. The SRs affect human health, such as cancer, blood pressure, heart attack, brain waves, and the nervous system (Cherry 2002; Mitsutakea et al. 2005). SR anomalies may help early detection of earthquakes (Ohta et al. 2006). Its intensity is largely modulated by fluctuations in the number and intensities of lightning flashes worldwide. There are intraseasonal (20–30 days) fluctuations in SR data (Fullekrug and Fraser-Smith 1996) because of the global connection between the MJO and lightning. As anomalous SR intensity undergoes its intraseasonal cycle, there is a systematic eastward shift of anomalous convective activity from tropical South America to the western Pacific (Anyamba et al. 2000), consistent with the eastward propagation pattern of the MJO. Maximum

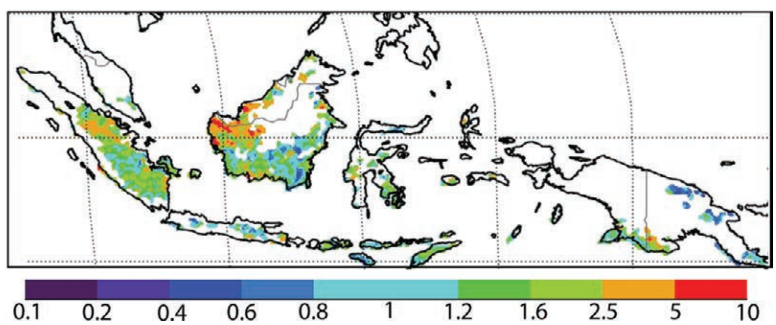

Fig. 6. Ratio of fire detections for MJO phases 5–8 over 1–4 in June–November (from Reid et al. 2012).

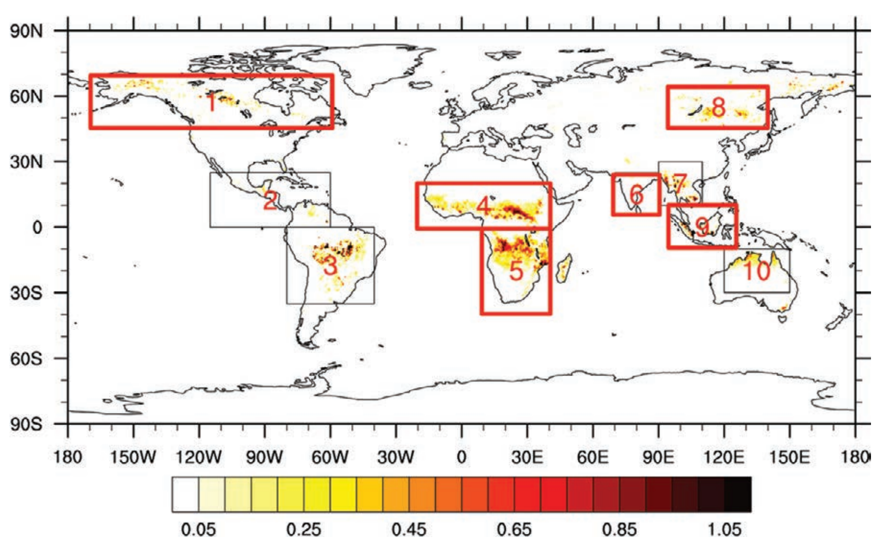

Fig. 7. Total fire carbon emission (g C m² day⁻¹) based on data of Mu et al. (2011). Red boxes indicate regions where fire emission fluctuates substantially with MJO phases.

SR intensity occurs when maximum convection is over Africa. Minimum SR intensity occurs when convection is maximum over the western Pacific and minimum over Africa.

SURFACE TEMPERATURE. In East Asia, two-thirds of extreme cold surges with temperature reductions greater than two standard deviations occur when MJO convection is over the Indian Ocean (Jeong et al. 2005). Combined effects of the MJO and other factors (e.g., the Arctic Oscillation) might have led to an extreme cold surge with record-breaking snowfall in Korea (Park et al. 2010). In general, the MJO tends to prevent weak cold surges from penetrating southward into the subtropics and tropics (Chang et al. 2005). During a cold year of ENSO, however, an MJO event with its convection center stalled over Sumatra might have resulted in an extreme cold event that broke a 50-yr record of minimum daily temperature and duration of large negative temperature anomalies (>1 standard deviation) over Southeast Asia in February 2008 (Hong and Li 2009).

When the MJO convection center is over the Indian Ocean, anomalies in surface air temperature 2°–5°C above normal tend to occur in central/northern Alaska and central/eastern Canada. As the MJO convection moves eastward, warm anomalies shift northward in Canada and are replaced by cold anomalies over Alaska. It is suggested that such temperature fluctuations are related to warm advection associated with the Rossby wave train emanated from enhanced convection of the MJO (Vecchi and Bond 2004; Lin and Brunet 2009). The MJO, through its influences on the Artic Oscillation (see discussion below), can induce surface temperature fluctuations of more than 1°C over a large portion of the northern hemispheric high latitudes (L'Heureux and Higgins 2008). MJO influences on wintertime (December–February) surface air temperature over the United States are illustrated in Fig. 9. In the northeastern and the Great Lake areas, surface air temperature may fluctuate over 5°C between MJO phases 1 and 5. Over northern Argentina, minimum winter (June–September) surface air temperature fluctuates by 6°C between MJO phases 3 and 6 (Naumann and Vargas 2010).

MJO influences on wintertime surface air temperatures extend to the Arctic, with warming (cooling) in MJO phase 5 (1) because of enhanced (reduced) poleward-propagating Rossby waves and eddy heat flux (Yoo et al. 2012). It is interesting that surface warming induced by the MJO attains a spatial pattern (stronger over land than over water) similar to the high-latitude decadal warming. This warming pattern manifests the Arctic amplification of global climate change in the past century (Yoo et al. 2011).

EXTRATROPICAL CLIMATE MODES. It has been known that extended weather forecast for the extratropics critically depends on tropical intraseasonal variability (Ferranti et al. 1990). Recent studies have identified connections between the MJO and several extratropical climate modes. The North Atlantic Oscillation (NAO) is the most dominant and recurrent pattern of atmospheric variability in the winter season of the Northern Hemisphere. Its sea level pressure pattern and associated surface temperature, precipitation, wind, and winter storms fluctuate on time scales ranging from days to decades, affecting the economy and ecosystems over a broad region at the northern middle and high latitudes (Hurrell et al. 2003). Lin et al. (2009) found a significant amplification of a positive (negative) phase of the NAO (25%–41% of its mean) about 5–15 days

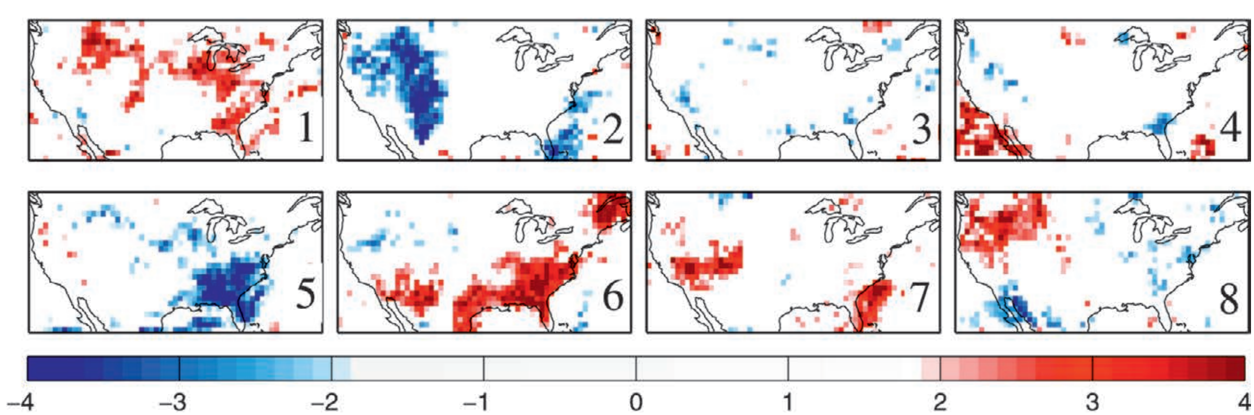

Fig. 8. Summer (June–September) lightning frequency rank-order anomalies (z scores) stratified by RMM phases (denoted in lower-right corner). Red (blue) shading denotes areas of enhanced (suppressed) lighting activity for each RMM phase exceeding the 95% confidence interval (from Abatzoglou and Brown 2009).

after depressed (enhanced) convection of the MJO reaches the central Pacific. They suggested that MJO influences on the NAO take place through northward momentum transport by Rossby wave dispersion from the tropical Pacific to the extratropical North Atlantic. A statistical model based on the connection between the MJO and NAO predicts the daily sign of the wintertime NAO with a success rate of about 70% at a lead time of 9–13 days (Cassou 2008).

The MJO also influences the Arctic Oscillation (AO), which is also known as the northern annular mode (Thompson and Wallace 2000). Anomalous zonal-mean westerlies at about 55°N and anomalous zonal-mean easterlies at about 35°N (contraction of the midlatitude jet) define the positive polarity of the AO, while the opposite signs (expansion of the midlatitude jet) define the negative polarity. More frequent midlatitude cold-air outbreaks tend to occur during the negative polarity of the AO than its positive polarity (Higgins et al. 2000; Thompson and Wallace 2001). Zhou and Miller (2005) found that, when MJO convection is enhanced (suppressed) over the Indian Ocean, the positive (negative) polarity of the wintertime AO is twice as likely to occur as the opposite polarity. L'Heureux and Higgins (2008) showed that the number of days with the positive AO polarity is large when MJO convection center is in the Eastern Hemisphere, especially over the Maritime Continent; in contrast, the number of days with the negative AO polarity is large when MJO convection in the Eastern Hemisphere is suppressed (phases 7 and 8). In November–March, 18%–21% of the AO variance in 1000-hPa geopotential height is related to the MJO. Both studies demonstrated that the Rossby wave train excited by MJO convection and propagating from the tropical Pacific into the extratropics is instrumental to the corresponding variability of the AO.

The Pacific and North American (PNA) teleconnection pattern is a prominent climate variability in boreal winter (Wallace and Gutzler 1981). In its positive phase, positive anomalies in 700–300-hPa heights are over Hawaii and western North America, negative anomalies are over south of the Aleutian Islands and the eastern United States, positive (negative) anomalies in temperatures are over western North America (across the south-central and southeastern

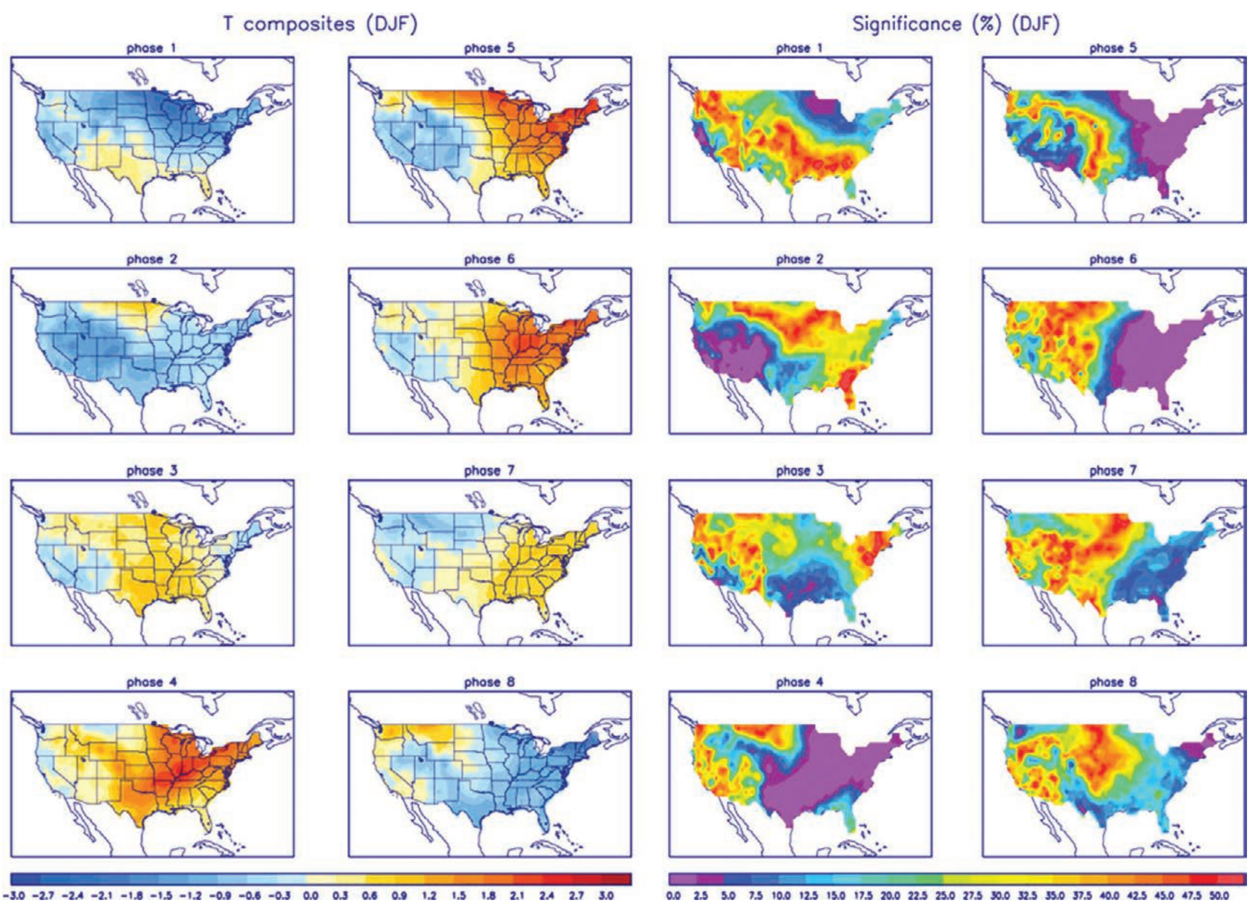

Fig. 9. December–February composites of surface air temperature anomalies (°C) for each MJO phase (from Zhou et al. 2012).

United States), and positive (negative) precipitation anomalies are over the Gulf of Alaska extending into the U.S. Pacific Northwest (over the upper U.S. Midwest). Interannually, the positive (negative) phase of the PNA tends to occur during a warm or El Niño (cold, or La Niña) event. Intraseasonally, the positive (negative) phase of the PNA pattern is most likely to occur during MJO phases 7–1 (3–5) when MJO convection is inactive (active) over the region from the Bay of Bengal to the western Pacific. This MJO–PNA connection explains about 30% of the emergence of the PNA pattern (Mori and Watanabe 2008; Lin et al. 2009; Johnson and Feldstein 2010). Propagation of Rossby wave trains from anomalous convection of the MJO has been identified as the main mechanisms for this MJO–PNA connection.

By the similar mechanism of Rossby wave trains, the MJO also affects the southern annular mode (SAM) or Antarctic Oscillation (AAO). In austral winter, negative (positive) phases of the AAO tend to occur when MJO convection is enhanced (suppressed) over the central Pacific (Carvalho et al. 2005). Meanwhile, the SAM reaches its maximum positive polarity seven days after MJO convection peaks over the equatorial Indian Ocean. MJO enhances surface westerly wind associated with the SAM over almost the entire latitude circle at 60°S and accelerates the Antarctic circumpolar transport (Matthews and Meredith 2004).

ENSO. The possible role of the MJO in ENSO has been reviewed by Zhang (2005) and Lau (2012). Here, a brief synthesis and updates are given.

Observational evidence of MJO influences on ENSO comes from both case studies and statistics. Recent major ENSO warning events (El Niño) were preceded by extraordinarily strong episodes of the MJO (McPhaden 1999, 2004, 2008). ENSO warming in the eastern Pacific tends to be preceded by enhanced MJO activities (Zhang and Gottschalck 2002) and their associated westerly wind events (Seiki and Takayabu 2007a) by 6–12 months. This suggests that MJO activities in boreal spring are crucial to ENSO warm events (Hendon et al. 2007).

It has been repeatedly demonstrated that prescribed wind perturbations of the MJO derived from observations can help coupled models reproduce better ENSO cases (Lengaigne et al. 2004) and statistics (Zavala-Garay et al. 2008; Kapur et al. 2011). The importance of feedback from ENSO SST to stochastic forcing ("multiplicative noise") has recently been recognized (Jin et al. 2007). Many ENSO properties, such as its strength, period, asymmetry, and prediction depend on SST feedback to high-frequency surface wind (Eisenman et al. 2005; Perez et al. 2005; Gebbie and Tziperman 2009). The MJO is not an exception (Seiki and Takayabu 2007b). Simulated ENSO is sensitive to how its SST anomalies feed back to the zonal extent of the eastward MJO propagation into the central and eastern Pacific (Kapur and Zhang 2012).

Skills of global coupled climate models to simulate ENSO appear to be related to their capability of producing MJO westerly wind events over the western Pacific (Shi et al. 2009; Seiki et al. 2011). Improved model representations of physics that lead to better MJO simulations may also yield better ENSO statistics (Wu et al. 2007; Neale et al. 2008; Stan et al. 2010).

INDIAN OCEAN DIPOLE. The Indian Ocean dipole (IOD; Saji et al. 1999), with an ENSO-like zonal gradient in SST, is the dominant interannual variability in the tropical Indian Ocean. In the positive phase of IOD, negative SST anomalies occur in the eastern Indian Ocean offshore Sumatra, which reach the maximum during boreal fall. Corresponding anomalies in the atmospheric circulation have a broad impact in the region (Webster et al. 1999).

The MJO has been suggested to be one of the mechanisms for IOD. A diagnosis of IOD in 2003, 2006, and 2007 (Rao et al. 2008) indicated that the MJO might have helped initiation of IOD if its convectively suppressed phase occurs over the Indian Ocean in May–June. Easterlies associated with convectively suppressed phases of the MJO can causes shoaling of the thermocline in the eastern Indian Ocean through anomalous upwelling oceanic Kelvin waves. On the other hand, downwelling oceanic Kelvin waves that deepen the thermocline may act to help terminate IOD if they are generated by anomalous surface westerly wind associated with convectively active phases of the MJO after IOD is initiated, similar to the process by which MJO affects the onset of ENSO warm events. By the same token, an IOD mature phase can sustain itself only in the absence of strong MJO events (Rao and Yamagata 2004). Modeling studies appear to yield similar results (Rao et al. 2007; Waliser et al. 2003b).

WYRTKI JETS. Narrow (2°N–2°S), strong (0.5–2 m s^{-1}) ocean surface (0–100 m) eastward currents along the equator across the Indian Ocean during the transition periods between the two monsoon seasons (April–May and October–November) are known as the Wyrtki jets (Wyrtki 1973). The only eastward equatorial surface currents in the world oceans, the Wyrtki jets cast substantial effects on the region. They transport salinity, heat, and mass eastward; deepen the mixed layer and thermocline depth, raise the sea level, and increase surface temperature in the eastern equatorial Indian Ocean; induce eastern boundary waves that move toward higher latitudes; and are closely related to the equatorial undercurrent, subsurface current, entrainment, and the IOD (Hastenrath et al. 1993; Schott and McCreary 2001; Han et al. 2004; Nagura and McPhaden 2010). In addition to their semiannual variability related to the seasonal transition of the monsoon wind (Knox 1976), the Wyrtki jets also fluctuate on intraseasonal time scales (McPhaden 1982). Surface westerly wind associated with the MJO generates intraseasonal fluctuations of the Wyrtki jets during spring and fall and also causes intraseasonal enhancement of the equatorial eastward surface current during summer and winter (Senan et al. 2003; Masumoto et al. 2005; Sengupta et al. 2007), which will be referred to also as the Wyrtki jets. Intraseasonal variability of the Wyrtki jets exhibits two spectral peaks at 30–60 and 90 days. The 30–60-day peak results directly from MJO forcing. The 90-day peak comes from resonant excitation of the second-baroclinic waves by the MJO wind at its low-frequency spectral end (Han 2005) and from interference between directly forced and reflected ocean waves (Nagura and McPhaden 2012). MJO forcing to the Wyrtki jets can also rectify into the seasonal to interannual time scales (Han et al. 2004). The intraseasonal peak of the Wyrtki jets is often greater than its seasonal amplitudes.

INDONESIAN THROUGHFLOW. The Indonesian Throughflow (ITF) is the main artery transporting heat and mass from the Pacific to Indian Oceans (Wyrtki 1987). It undergoes intraseasonal, as well as annual and interannual, fluctuations. In many parts of the Indonesian Seas, intraseasonal spectral peaks at 50–60 days were found in upper-ocean (0–500 m) currents (Molcard et al. 1996), as well as in sea surface temperature (Ffield and Gordon 1996), sea level (Arief and Murray 1996), surface dynamic height (Bray et al. 1997), and subsurface temperature and salinity (Kashino et a. 1999). These observed intraseasonal signals were suggested to be related to the MJO. A detailed modeling study (Qiu et al. 1999) identified two areas where intraseasonal fluctuations in the ITF might be attributed to the MJO: intraseasonal signals in the ITF near the Sumatra–Java coasts of the eastern Indian Ocean are related to those in the zonal wind over the central equatorial Indian Ocean, possibly through eastward propagation of MJO-forced oceanic Kelvin waves (Zhou and Murtugudde 2010), and intraseasonal signals in the Timor Straits are forced by intraseasonal fluctuations in local wind. In a GCM simulation, intraseasonal fluctuation in the ITF forced by the MJO is of the same strength as its annual and interannual variability (Waliser et al. 2003b). Because of the important function of the ITF in the heat balance and thermocline circulation of not only the Indian Ocean but also the global oceans (Godfrey 1996), MJO's influence on the ITF is another example of its role in global climate.

OTHER EFFECTS. The MJO also cast significant influences on many other phenomena in the Earth system. They can only be briefly mentioned in this article because of its length limitation. Some of them have been reviewed in detail elsewhere as cited below.

The MJO, by affecting air–sea fluxes, modulates upper-ocean temperature and salinity, the depths of the mixed layer and thermocline, and generated equatorial ocean waves (see reviews by Zhang 2005; Kessler 2012; Hendon 2012; Duvel 2012).

Through its component of surface zonal winds, the MJO modulates the momentum exchange between the atmosphere and the solid Earth. In consequence, the Earth angular momentum fluctuates in concert with MJO activities and so does the length of the day. A review on this subject was given by Chao and Salstein (2012).

MJO deep convection casts substantial influences on the variability in upper-tropospheric and lower-stratospheric water vapor (Mote et al. 2000; Sassi et al. 2002; Zhan et al. 2006) and cloud ice water content (Schwartz et al. 2008) as part of its effect on the atmospheric water cycle (Waliser et al. 2009).

The MJO can induce intraseasonal fluctuations in atmospheric CO (Wong and Dessler 2007), CO_2 (Li et al. 2010), O_3 (K.-F. Li et al. 2012), and upper-ocean chlorophyll (Jin et al. 2013) and nutrients (Resplandy et al. 2009). A review on this subject was given by Tian and Waliser (2012).

The MJO modulates tropospheric aerosol (see a review by Tian and Waliser 2012). Over the equatorial Indian Ocean, surface aerosol undergo a regime transition from dominance by submicrometer sulfate aerosol of continental origin before a local MJO convectively active period to dominance by sea spray afterward when surface wind becomes strong (DeWitt et al. 2013).

In many areas of the Indian and Pacific Oceans, sea level fluctuates intraseasonally with amplitudes more than 10 cm, mainly because of MJO-generated equatorial Kelvin and Rossby waves and coastal waves (Oliver and Thompson 2010).

In addition to the Wyrtki jets, the MJO also induces intraseasonal fluctuations in other ocean currents, such as the Somali current (Mysak and Mertz 1984) and the Indian Ocean south equatorial current (Zhou et al. 2008).

When MJO convection moves from the Indian Ocean to the western Pacific, tropical (10°S–10°N) mean cirrus fraction in the tropopause transition layer (TTL) doubles with its maximum over equatorial Africa and South America (Virts and Wallace 2010). Meanwhile, the tropical tropopause rises at most longitudes (Son and Lee 2007) in addition to regions near the MJO convection center (Madden and Julian 1972), and tropopause (cold point) temperature drops more than 2°C (Kiladis et al. 2001; Zhou and Holton 2002). The largest perturbations occur in the subtropical cyclonic vortices on the polar sides of the MJO convection center (Tian et al. 2012).

The MJO influences ITCZ breakdown in the Pacific (Wang and Magnusdottir 2006). Convective initiation of the MJO over the Indian Ocean interrupts the ITCZ south of the equator (Yoneyama et al. 2013). Precipitation in the Atlantic ITCZ is enhanced when the MJO convection center is over either the Indian or western Pacific Ocean but reduced when it is over the Maritime Continent (see Fig. SB2 in the sidebar).

The MJO affects global atmospheric circulations and tropical waves (see a review by Roundy 2012).

MJO influences on weather depend on the mean state, which varies with the season and other climate variability such as ENSO (Roundy et al. 2010; Moon et al. 2011; C. Y. Li et al. 2012).

CONCLUDING REMARKS. There is hardly another phenomenon that is globally connected to both weather and climate as broadly as the MJO. The broad connections between the MJO and many types of weather and climate events are strong testaments to the realization that the societal need of weather and climate prediction cannot be met without advancing our understanding of the MJO and without improving our ability of predicting the MJO (Walier et al. 2003) and associated teleconnections (Vitart and Molteni 2010). While considerable progress has been made in the study of the MJO (Wang 2012; Sperber et al. 2012; Majda and Stechmann 2012; Zhang 2012) since it was first documented by Madden and Julian (1971, 1972), our understanding of it is still incomplete and its prediction skill is still limited (Waliser 2012). It is a great challenge for Earth system models to reproduce the observed connections between the MJO and weather/climate events. Such a capability is essential for any Earth system model to serve as a credible tool for simulation and prediction of weather and climate, especially their extremes. The endeavor of understanding and predicting weather, climate, and their extremes must be achieved with the MJO and intraseasonal variability in general included as the integrated part of the weather–climate continuum.

ACKNOWLEDGMENTS. The author thanks Duane Waliser and two anonymous reviewers for their careful and constructive comments on the submitted manuscript of this article. He is also grateful to Weiqing Han, Charles Jones, Hai Lin, Eric Maloney, and Matthew Wheeler for their comments and suggestions on certain parts of the manuscript. Thanks also go to Jian Ling and David Zermeno for their help of making some of the figures. The effort of writing this article was supported by grants from the National Science Foundation (AGS-1062202), the Office of Science (BER) of the US Department of Energy (DE-SC0006808, DE-SC0008568), the National Oceanic and Atmospheric Administration (GC09-330a), and the Office of Naval Research (N000141210984).

REFERENCES

Abatzoglou, J. T., and T. J. Brown, 2009: Influence of the Madden–Julian oscillation on summertime cloud-to-ground lightning activity over the continental United States. *Mon. Wea. Rev.,* **137,** 3596–3601.

Alaka, G. J., and E. D. Maloney, 2012: The Madden–Julian oscillation influence on upstream African easterly wave precursor disturbances during boreal summer. *J. Climate,* **25,** 3219–3236.

Aldrian, E., 2008: Dominant factors of Jakarta's three largest floods. *J. Hidrosfir Indones.,* **3,** 105–112.

Anyamba, E., E. Williams, J. Susskind, A. Fraser-Smith, and M. Fullekrug, 2000: The manifestation of the Madden–Julian oscillation in global deep convection and in the Schumann resonance intensity. *J. Atmos. Sci.,* **57,** 1029–1044.

Arief, D., and S. P. Murray, 1996: Low-frequency fluctuations in the Indonesian throughflow through Lombok Strait. *J. Geophys. Res.,* **101** (C5), 12 455–12 464.

Barlow, M., 2012: Africa and west Asia. *Intraseasonal Variability of the Atmosphere–Ocean Climate System,* 2nd ed. W. K.-M. Lau and D. E. Waliser, Eds., Springer, 477–496.

——, M. Wheeler, B. Lyon, and H. Cullen, 2005: Modulation of daily precipitation over Southwest Asia by the Madden–Julian oscillation. *Mon. Wea. Rev.,* **133,** 3579–3594.

Barrett, B. S., J. F. Carrasco, and A. P. Testino, 2012: Madden–Julian oscillation (MJO) modulation of atmospheric circulation and Chilean winter precipitation. *J. Climate,* **25,** 1678–1688.

Becker, E. J., E. Hugo Berbery, and R. W. Higgins, 2011: Modulation of cold-season U.S. daily precipitation by the Madden–Julian oscillation. *J. Climate,* **24,** 5157–5166.

Belanger, J. I., J. A. Curry, and P. J. Webster, 2010: Predictability of North Atlantic tropical cyclone activity on intraseasonal time scales. *Mon. Wea. Rev.,* **138,** 4362–4374.

Bessafi, M., and M. C. Wheeler, 2006: Modulation of south Indian Ocean tropical cyclones by the Madden–Julian oscillation and convectively coupled equatorial waves. *Mon. Wea. Rev.,* **134,** 638–656.

Bond, N. A., and G. A. Vecchi, 2003: The influence of the Madden–Julian oscillation on precipitation in Oregon and Washington. *Wea. Forecasting,* **18,** 600–613.

Bray, N. A., S. E. Wijffels, J. C. Chong, M. Fieux, S. Hautala, G. Meyers, and W. M. L. Morawitz, 1997: Characteristics of the Indo-Pacific throughflow in the eastern Indian Ocean. *Geophys. Res. Lett.,* **24,** 2569–2572.

Brown, A., S. Milton, M. Cullen, B. Golding, J. Mitchell, and A. Shelly, 2012: Unified modeling and prediction of weather and climate: A 25-year journey. *Bull. Amer. Meteor. Soc.,* **93,** 1865–1877.

Brunet, G., and Coauthors, 2010: Collaboration of the Weather and climate communities to advance subseasonal-to-seasonal prediction. *Bull. Amer. Meteor. Soc.,* **91,** 1397–1406.

Camargo, S. J., M. C. Wheeler, and A. H. Sobel, 2009: Diagnosis of the MJO modulation of tropical cyclogenesis using an empirical index. *J. Atmos. Sci.,* **66,** 3061–3074.

Carvalho, L. M. V., C. Jones, and B. Liebmann, 2004: The South Atlantic convergence zone: Intensity, form, persistence, and relationships with intraseasonal to interannual activity and extreme rainfall. *J. Climate,* **17,** 88–108.

——, and ——, and T. Ambrizzi, 2005: Opposite phases of the Antarctic Oscillation and relationships with intraseasonal to interannual activity in the tropics during the austral summer. *J. Climate,* **18,** 702–718.

Cassou, C., 2008: Intraseasonal interaction between the Madden-Julian oscillation and the North Atlantic Oscillation. *Nature,* **455,** 523–527.

Chang, C.-P., P. A. Harr, and H.-J. Chen, 2005: Synoptic disturbances over the equatorial South China Sea and western maritime continent during boreal winter. *Mon. Wea. Rev.,* **133,** 489–503.

——, N.-C. Lau, R. H. Johnson, and M. Jiao, 2011: Bridging weather and climate in research and forecasts of the global monsoon system. *Bull. Amer. Meteor. Soc.,* **92,** 369–373.

Chao, B. F., and D. A. Salstein, 2012: Mass, momentum, and geodynamics. *Intraseasonal Variability of the Atmosphere–Ocean Climate System,* 2nd ed. W. K.-M. Lau and D. E. Waliser, Eds., Springer, 271–296.

Charney, J. G., and J. Shukla, 1977: Predictability of monsoons. *Proc. Joint IUTAM/IUGG Symp. on Monsoon Dynamics,* New Delhi, India.

Cherry, N. J., 2002: Schumann resonances, a plausible biophysical mechanism for the human health effects of solar/geomagnetic activity. *Nat. Hazards,* **26,** 279–331.

DeMott, C. A., and S. A. Rutledge, 1998a: The vertical structure of TOGA COARE convection. Part I: Radar echo distributions. *J. Atmos. Sci.,* **55,** 2730–2747.

——, and ——, 1998b: The vertical structure of TOGA COARE convection. Part II: Modulating influences and implications for diabatic heating. *J. Atmos. Sci.,* **55,** 2748–2762.

Dettinger, M. D., 2011: Climate change, atmospheric rivers and floods in California—A multimodel analysis of storm frequency and magnitude changes. *J. Amer. Water Resour. Assoc.,* **47,** 514–523, doi:10.1111/j.1752-1688.2011.00546.x.

DeWitt, H. L., D. J. Coffman, K. J. Schulz, W. A. Brewer, T. S. Bates, and P. K. Quinn, 2013: Atmospheric aerosol properties over the equatorial Indian Ocean and the impact of the Madden-Julian oscillation. *J. Geophys. Res.,* **118,** 5736–5749, doi:10.1002/jgrd.50419.

Dole, R. M., 2008: Linking weather and climate. *Synoptic-Dynamic Meteorology and Weather Analysis and Forecasting: A Tribute to Fred Sanders, Meteor. Monogr.,* No. 33, Amer. Meteor. Soc., 297–348.

Donald, A., H. Meinke, B. Power, A. de H. N. Maia, M. C. Wheeler, N. White, R. C. Stone, and J. Ribbe, 2006: Near-global impact of the Madden-Julian Oscillation on rainfall, *Geophys. Res. Lett.,* **33,** L09704, doi:10.1029/2005GL025155.

Duvel, J. P., 2012: Oceans and air-sea interaction. *Intraseasonal Variability of the Atmosphere–Ocean Climate System*, 2nd ed. W. K.-M. Lau and D. E. Waliser, Eds., Springer, 513–536.

Eisenman, I., L. Yu, and E. Tziperman, 2005: Westerly wind bursts: ENSO's tail rather than the dog? *J. Climate,* **18,** 5224–5238.

Ferranti, L., T. N. Palmer, F. Molteni, and K. Klinker, 1990: Tropical–extratropical interaction associated with the 30–60-day oscillation and its impact on medium and extended range prediction. *J. Atmos. Sci.,* **47,** 2177–2199.

Ferreira, R. N., W. H. Schubert, and J. J. Hack, 1996: Dynamical aspects of twin tropical cyclones associated with the Madden–Julian oscillation. *J. Atmos. Sci.,* **53,** 929–945.

Ffield, A., and A. L. Gordon, 1996: Tidal mixing signatures in the Indonesian seas. *J. Phys. Oceanogr.,* **26,** 1924–1937.

Frank, W. M., and P. E. Roundy, 2006: The role of tropical waves in tropical cyclogenesis. *Mon. Wea. Rev.,* **134,** 2397–2417.

Fullekrug, M., and A. C. Fraser-Smith, 1996: Further evidence for a global correlation of the Earth–ionosphere cavity resonances. *Geophys. Res. Lett.,* **23,** 2773–2776.

Gebbie, G., and E. Tziperman, 2009: Predictability of SST-modulated westerly wind bursts. *J. Climate,* **22,** 3894–3909.

Godfrey, J. S., 1996: The effect of the Indonesian throughflow on ocean circulation and heat exchange with the atmosphere: A review. *J. Geophys. Res.,* **101** (C5), 12 217–12 237.

Goswami, B. N., 2012: South Asian monsoon. *Intraseasonal Variability of the Atmosphere–Ocean Climate System,* 2nd ed. W. K.-M. Lau and D. E. Waliser, Eds., Springer, 21–72.

Gottschalck, J., and Coauthors, 2010: A framework for assessing operational Madden–Julian oscillation forecasts: A CLIVAR MJO Working Group project. *Bull. Amer. Meteor. Soc.,* **91,** 1247–1258.

Grimm, A. M., and P. L. Silva Dias, 1995: Analysis of tropical–extratropical interactions with influence functions of a barotropic model. *J. Atmos. Sci.,* **52,** 3538–3555.

Guan, B., D. E. Waliser, N. P. Molotch, E. J. Fetzer, and P. J. Neiman, 2012: Does the Madden–Julian oscillation influence wintertime atmospheric rivers and snowpack in the Sierra Nevada? *Mon. Wea. Rev.,* **140,** 325–342.

Hall, J. D., A. J. Matthews, and D. J. Karoly, 2001: The modulation of tropical cyclone activity in the Australian region by the Madden–Julian oscillation. *Mon. Wea. Rev.,* **129,** 2970–2982.

Han, W., 2005: Origins and dynamics of the 90-day and 30–60-day variations in the equatorial Indian Ocean. *J. Phys. Oceanogr.,* **35,** 708–728.

——, P. Webster, R. Lukas, P. Hacker, and A. Hu, 2004: Impact of atmospheric intraseasonal variability in the Indian Ocean: Low-frequency rectification in equatorial surface current and transport. *J. Phys. Oceanogr.,* **34,** 1350–1372.

Hastenrath, S., A. Nicklis, and L. Greischar, 1993: Atmospheric–hydrospheric mechanisms of climate anomalies in the western equatorial Indian Ocean. *J. Geophys. Res.,* **98** (C11), 20 219–20 235.

He, J., H. Lin, and Z. Wu, 2011: Another look at influences of the Madden-Julian oscillation on the wintertime East Asian weather. *J. Geophys. Res.,* **116,** D03109, doi:10.1029/2010JD014787.

Heinlein, R., 1973: *Time Enough for Love.* G.P. Putnam's Sons, 605 pp.

Hendon, H. H., 2012: Air-sea interaction. *Intraseasonal Variability of the Atmosphere–Ocean Climate System,* 2nd ed. W. K.-M. Lau and D. E. Waliser, Eds., Springer, 247–270.

——, M. C. Wheeler, and C. Zhang, 2007: Seasonal dependence of the MJO–ENSO relationship. *J. Climate,* **20,** 531–543.

Herbertson, A. J., 1901: *Outlines of Physiography: An Introduction to the Study of the Earth.* Edward Arnold, 312 pp.

Higgins, R. W., A. Leetmaa, Y. Xue, and A. Barnston, 2000: Dominant factors influencing the seasonal predictability of U.S. precipitation and surface air temperature. *J. Climate,* **13,** 3994–4017.

Ho, C.-H., J.-H. Kim, J.-H. Jeong, H.-S. Kim, and D. Chen, 2006: Variation of tropical cyclone activity in the south Indian Ocean: El Niño–Southern Oscillation and Madden-Julian Oscillation effects. *J. Geophys. Res.,* **111,** D22101, doi:10.1029/2006JD007289.

Hong, C.-C., and T. Li, 2009: The extreme cold anomaly over Southeast Asia in February 2008: Roles of ISO and ENSO. *J. Climate,* **22,** 3786–3801.

Hsu, H.-H., 2012: East Asian monsoon. *Intraseasonal Variability of the Atmosphere–Ocean Climate System.* 2nd ed. W. K.-M. Lau and D. E. Waliser, Eds., Springer, 73–110.

Hurrell, J. W., Y. Kushnir, G. Ottersen, and M. Visbeck, 2003: An overview of the North Atlantic Oscillation. *North Atlantic Oscillation: Climate Significance and Environmental Impact, Geophys. Monogr.,* Vol. 134, Amer. Geophys. Union, 1–35.

——, G. A. Meehl, D. Bader, T. Delworth, B. Kirtman, and B. Wielicki, 2009: A unified modeling approach to climate system prediction. *Bull. Amer. Meteor. Soc.,* **90,** 1819–1832.

Janicot, S., F. Mounier, N. M. J. Hall, S. Leroux, B. Sultan, and G. N. Kiladis, 2009: Dynamics of the West African monsoon. Part IV: Analysis of 25–90-day variability of convection and the role of the Indian monsoon. *J. Climate,* **22,** 1541–1565.

——, and Coauthors, 2011: Intraseasonal variability of the West African monsoon. *Atmos. Sci. Lett.,* **12,** 58–66.

Jeong, J.-H., C.-H. Ho, B.-M. Kim, and W.-T. Kwon, 2005: Influence of the Madden-Julian Oscillation on wintertime surface air temperature and cold surges in East Asia. *J. Geophys. Res.,* **110,** D11104, doi:10.1029/2004JD005408.

——, B.-M. Kim, C.-H. Ho, and Y.-H. Noh, 2008: Systematic variation in wintertime precipitation in East Asia by MJO-induced extratropical vertical motion. *J. Climate,* **21,** 788–801.

Jia, X., L. J. Chen, F. M. Ren, and C. Y. Li, 2011: Impacts of the MJO on winter rainfall and circulation in China. *Adv. Atmos. Sci.,* **28,** 521–533, doi:10.1007/s00376-010-9118-z.

Jiang, X., M. Zhao, and D. E. Waliser, 2012: Modulation of tropical cyclones over the eastern Pacific by the intraseasonal variability simulated in an AGCM. *J. Climate,* **25,** 6524–6538.

Jin, D., D. E. Waliser, C. Jones, and R. Murtugudde, 2013: Modulation of tropical ocean surface chlorophyll by the Madden–Julian oscillation. *Climate Dyn.,* **40,** 39–58.

Jin, F.-F., L. Lin, A. Timmermann, and J. Zhao, 2007: Ensemble-mean dynamics of the ENSO recharge oscillator under state-dependent stochastic forcing. *Geophys. Res. Lett.,* **34,** L03807, doi:10.1029/2006GL027372.

Johnson, N. C., and S. B. Feldstein, 2010: The continuum of North Pacific sea level pressure patterns: Intraseasonal, interannual, and interdecadal variability. *J. Climate,* **23,** 851–867.

Jones, C., and L. M. V. Carvalho, 2012: Spatial–intensity variations in extreme precipitation in the contiguous United States and the Madden–Julian oscillation. *J. Climate,* **25,** 4849–4913.

——, D. E. Waliser, K. M. Lau, and W. Stern, 2004: Global occurrences of extreme precipitation events and the Madden–Julian oscillation: Observations and predictability. *J. Climate,* **17,** 4575–4589.

——, J. Gottschalck, L. M. V. Carvalho, and W. R. Higgins, 2011a: Influence of the Madden–Julian oscillation on forecasts of extreme precipitation in the contiguous United States. *Mon. Wea. Rev.,* **139,** 332–350.

——, L. M. V. Carvalho, J. Gottschalck, and W. Higgins, 2011b: The Madden–Julian oscillation and the relative value of deterministic forecasts of extreme precipitation in the contiguous United States. *J. Climate,* **24,** 2421–2428.

Juliá, C., D. A. Rahn, and J. A. Rutllant, 2012: Assessing the influence of the MJO on strong precipitation events in subtropical, semi-arid north-central Chile (30°S). *J. Climate,* **25,** 7003–7013.

Kapur, A., and C. Zhang, 2012: Multiplicative MJO forcing of ENSO. *J. Climate,* **25,** 8132–8147.

——, C. Zhang, J. Zavala-Garay, and H. H. Hendon, 2011: Role of stochastic forcing in ENSO in observations and a coupled GCM. *Climate Dyn.,* **38,** 87–107.

Kashino, Y., H. Watanabe, B. Herunadi, M. Aoyama, and D. Hartoyo, 1999: Current variability at the Pacific entrance of the Indonesian Throughflow. *J. Geophys. Res.,* **104** (C5), 11 021–11 035.

Keen, R. A., 1982: The role of cross-equatorial tropical cyclone pairs in the Southern Oscillation. *Mon. Wea. Rev.,* **110,** 1405–1416.

Kessler, W. S., 2012: The oceans. *Intraseasonal Variability of the Atmosphere–Ocean Climate System,* 2nd ed. W. K.-M. Lau and D. E. Waliser, Eds., Springer, 199–246.

Kiladis, G. N., K. H. Straub, G. C. Reid, and K. S. Gage, 2001: Aspects of interannual and intraseasonal variability of the tropopause and lower stratosphere. *Quart. J. Roy. Meteor. Soc.,* **127,** 1961–1983.

Klotzbach, P. J., 2010: On the Madden–Julian oscillation–Atlantic hurricane relationship. *J. Climate,* **23,** 282–293.

Knox, R. A., 1976: On a long series of measurements of Indian Ocean equatorial currents near Addu Atoll. *Deep-Sea Res.,* **23,** 211–221.

Kodama, Y.-M., M. Tokuda, and F. Murata, 2006: Convective activity over the Indonesian maritime continent during CPEA-I as evaluated by lightning activity and Q1 and Q2 profiles. *J. Meteor. Soc. Japan,* **84,** 133–149.

Laing, A. G., R. E. Carbone, and V. Levizzani, 2011: Cycles and propagation of deep convection over equatorial Africa. *Mon. Wea. Rev.,* **139,** 2832–2853.

Lau, W. K. M., 2012: El–Niño Southern Oscillation connection. *Intraseasonal Variability of the Atmosphere–Ocean Climate System,* 2nd ed. W. K.-M. Lau and D. E. Waliser, Eds., Springer, 297–334.

——, and D. E. Waliser, Eds., 2012: *Intraseasonal Variability of the Atmosphere–Ocean Climate System.* 2nd ed. Springer, 613 pp.

Lawrence, D. M., and P. J. Webster, 2002: The boreal summer intraseasonal oscillation: Relationship between northward and eastward movement of convection. *J. Atmos. Sci.,* **59,** 1593–1606.

Lengaigne, M., E. Guilyardi, J.-P. Boulanger, C. Menkes, P. Delecluse, P. Inness, J. Cole, and J. M. Slingo, 2004: Triggering of El Niño by westerly wind events in a coupled general circulation model. *Climate Dyn.,* **23,** 601–620.

Leroy, A., and M. C. Wheeler, 2008: Statistical prediction of weekly tropical cyclone activity in the Southern Hemisphere. *Mon. Wea. Rev.,* **136,** 3637–3654.

L'Heureux, M. L., and R. W. Higgins, 2008: Boreal winter links between the Madden–Julian oscillation and the Arctic Oscillation. *J. Climate,* **21,** 3040–3050.

Li, C. Y., W. Zhou, J. C. L. Chan, and P. Huang, 2012: Asymmetric modulation of the western North Pacific cyclogenesis by the Madden–Julian oscillation under ENSO conditions. *J. Climate,* **25,** 5374–5385.

Li, K.-F., B. Tian, D. E. Waliser, and Y. L. Yung, 2010: Tropical mid-tropospheric CO_2 variability driven by the Madden–Julian oscillation. *Proc. Natl. Acad. Sci. USA,* **107,** 19 171–19 175.

——, ——, ——, M. J. Schwartz, J. L. Neu, J. R. Worden, and Y. L. Yung, 2012: Vertical structure of MJO-related subtropical ozone variations from MLS, TES, and SHADOZ data. *Atmos. Chem. Phys.,* **12,** 425–436.

Liebmann, B., H. H. Hendon, and J. D. Glick, 1994: The relationship between tropical cyclones of the western Pacific and Indian Oceans and the Madden–Julian oscillation. *J. Meteor. Soc. Japan,* **72,** 401–412.

Lin, H., and G. Brunet, 2009: The influence of the Madden–Julian oscillation on Canadian wintertime surface air temperature. *Mon. Wea. Rev.,* **137,** 2250–2262.

——, G. Brunet, and J. Derome, 2009: An observed connection between the North Atlantic Oscillation and the Madden–Julian oscillation. *J. Climate,* **22,** 364–380.

Lorenz, E. N., 1975: Climatic predictability. *The Physical Basis of Climate and Climate Modeling,* GARP Publication Series, Vol. 16, World Meteorological Organization, 132–136.

Madden, R. A., and P. R. Julian, 1971: Detection of a 40-50 day oscillation in the zonal wind in the tropical Pacific. *J. Atmos. Sci.,* **28,** 702–708.

——, and ——, 1972: Description of global-scale circulation cells in the tropics with a 40-50 day period. *J. Atmos. Sci.,* **29,** 1109–1123.

Majda, A. J., and S. N. Stechmann, 2012: Multiscale theories for the MJO. *Intraseasonal Variability of the Atmosphere–Ocean Climate System,* 2nd ed. W. K.-M. Lau and D. E. Waliser, Eds., Springer, 549–565.

Maloney, E. D., and D. L. Hartmann, 2000a: Modulation of eastern North Pacific hurricanes by the Madden–Julian oscillation. *J. Climate,* **13,** 1451–1460.

——, and ——, 2000b: Modulation of hurricane activity in the Gulf of Mexico by the Madden–Julian oscillation. *Science,* **287,** 2002–2004.

——, and ——, 2001: The Madden–Julian oscillation, barotropic dynamics, and North Pacific tropical cyclone formation. Part I: Observations. *J. Atmos. Sci.,* **58,** 2545–2558.

——, and J. Shaman, 2008: Intraseasonal variability of the West African monsoon and Atlantic ITCZ. *J. Climate,* **21,** 2898–2918.

Marshall, A. G., D. Hudson, M. C. Wheeler, H. H. Hendon, and O. Alves, 2010: Assessing the simulation and prediction of rainfall associated with the MJO in the POAMA seasonal forecast system. *Climate Dyn.,* **37,** 2129–2141, doi:10.1007/s00382-010-0948-2.

Masumoto, Y., H. Hase, Y. Kuroda, H. Matsuura, and K. Takeuchi, 2005: Intraseasonal variability in the upper layer currents observed in the eastern equatorial Indian Ocean. *Geophys. Res. Lett.,* **32,** L02607, doi:10.1029/2004GL021896.

Matthews, A. J., 2004: Intraseasonal variability over tropical Africa during northern summer. *J. Climate,* **17,** 2427–2440.

——, and M. P. Meredith, 2004: Variability of Antarctic circumpolar transport and the southern annular mode associated with the Madden–Julian oscillation. *Geophys. Res. Lett.,* **31,** L24312, doi:10.1029/2004GL021666.

McPhaden, M. J., 1982: Variability in the central equatorial Indian Ocean. Part I: Ocean dynamics. *J. Mar. Res.,* **40,** 157–176.

——, 1999: Genesis and evolution of the 1997–98 El Niño. *Science,* **283,** 950–954.

——, 2004: Evolution of the 2002/03 El Niño. *Bull. Amer. Meteor. Soc.,* **85,** 677–695.

——, 2008: Evolution of the 2006-07 El Niño: The role of intraseasonal to interannual time scale dynamics. *Adv. Geosci.,* **14,** 219–230.

Mitsutakea, G., K. Otsukaa, M. Hayakawab, M. Sekiguchib, G. Cornélissenc, and F. Halberg, 2005: Does Schumann resonance affect our blood pressure? *Biomed. Pharmacother.,* **59** (Suppl.), S10–S14.

Mo, K. C., 2000: The association between intraseasonal oscillations and tropical storms in the Atlantic basin. *Mon. Wea. Rev.,* **128,** 4097–4107.

——, C. Jones, and J. N. Paegle, 2012: Pan-America. *Intraseasonal Variability of the Atmosphere–Ocean Climate System,* 2nd ed. W. K.-M. Lau and D. E. Waliser, Eds., Springer, 111–146.

Molcard, R., M. Fieux, and A. G. Ilahude, 1996: The Indo–Pacific throughflow in the Timor Passage. *J. Geophys. Res.,* **101** (C5), 12 411–12 420.

Moncrieff, M. W., D. E. Waliser, M. J. Miller, M. E. Shapiro, G. Asrar, and J. Caughey, 2012: Multiscale convective organization and the YOTC Virtual Global Field Campaign. *Bull. Amer. Meteor. Soc.,* **93,** 1171–1187.

Moon, J.-Y., B. Wang, and K.-J. Ha, 2011: ENSO regulation of MJO teleconnection. *Climate Dyn.,* **37,** 1133–1149.

——, ——, and ——, 2012: MJO modulation on 2009/10 winter snowstorms in the United States. *J. Climate,* **25,** 978–991.

Mori, M., and M. Watanabe, 2008: The growth and triggering mechanisms of the PNA: A MJO-PNA coherence. *J. Meteor. Soc. Japan,* **86,** 213–236.

Morita, J., Y. N. Takayabu, S. Shige, and Y. Kodama, 2006: Analysis of rainfall characteristics of the Madden-Julian oscillation using TRMM satellite data. *Dyn. Atmos. Oceans,* **42,** 107–126.

Mote, P. W., H. L. Clark, T. J. Dunkerton, R. S. Harwood, and H. C. Pumphrey, 2000: Intraseasonal variations of water vapor in the tropical upper troposphere and tropopause region. *J. Geophys. Res.,* **105** (D13), 17 457–17 470.

Mu, M., and Coauthors, 2011: Daily and hourly variability in global fire emissions and consequences for atmospheric model predictions of carbon monoxide. *J. Geophys. Res.,* **116,** D24303, doi:10.1029/2011JD016245.

Mysak, L. A., and G. J. Mertz, 1984: A 40- to 60-day oscillation in the source region of the Somali Current during 1976. *J. Geophys. Res.,* **89** (C1), 711–715.

Nagura, M., and M. J. McPhaden, 2010: Dynamics of zonal current variations associated with the Indian Ocean dipole. *J. Geophys. Res.,* **115,** C11026, doi:10.1029/2010JC006423.

——, and ——, 2012: The dynamics of wind-driven intraseasonal variability in the equatorial Indian Ocean. *J. Geophys. Res.,* **117,** C02001, doi:10.1029/2011JC007405.

Naumann, G., and W. M. Vargas, 2010: Joint diagnostic of the surface air temperature in southern South America and the Madden–Julian oscillation. *Wea. Forecasting,* **25,** 1275–1280.

Neale, R. B., J. H. Richter, and M. Jochum, 2008: The impact of convection on ENSO: From a delayed oscillator to a series of events. *J. Climate,* **21,** 5904–5924.

Ohta, K., N. Watanabe, and M. Hayakawa, 2006: Survey of anomalous Schumann resonance phenomena observed in Japan in possible association with earthquakes in Taiwan. *Phys. Chem. Earth,* **31,** 397–402.

Oliver, E. C. J., and K. R. Thompson, 2010: Madden-Julian oscillation and sea level: Local and remote forcing. *J. Geophys. Res.,* **115,** C01003, doi:10.1029/2009JC005337.

Park, T.-W., C.-H. Ho, S. Yang, and J.-H. Jeong, 2010: Influences of Arctic Oscillation and Madden-Julian oscillation on cold surges and heavy snowfalls over Korea: A case study for the winter of 2009–2010. *J. Geophys. Res.,* **115,** D23122, doi:10.1029/2010JD014794.

Perez, C. L., A. M. Moore, J. Zavala-Garay, and R. Kleeman, 2005: A comparison of the influence of additive and multiplicative stochastic forcing on a coupled model of ENSO. *J. Climate,* **18,** 5066–5085.

Pohl, B., and P. Camberlin, 2006a: Influence of the Madden–Julian Oscillation on East African rainfall. Part I: Intraseasonal variability and regional dependency. *Quart. J. Roy. Meteor. Soc.,* **132,** 2521–2539.

——, and P. Camberlin, 2006b: Influence of the Madden–Julian Oscillation on East African rainfall. II: March–May season extremes and interannual variability. *Quart. J. Roy. Meteor. Soc.,* **132,** 2541–2559.

Pyne, S. J., P. L. Andrews, and R. D. Laven, 1996: *Introduction to Wildland Fire.* John Wiley and Sons, 769 pp.

Qiu, B., M. Mao, and Y. Kashino, 1999: Intraseasonal variability in the Indo-Pacific Throughflow and the regions surrounding the Indonesian Seas. *J. Phys. Oceanogr.,* **29,** 1599–1618.

Ralph, F. M., P. J. Neiman, G. N. Kiladis, K. Weickmann, and D. W. Reynolds, 2011: A multiscale observational case study of a Pacific Atmospheric river exhibiting tropical–extratropical connections and a mesoscale frontal wave. *Mon. Wea. Rev.,* **139,** 1169–1189.

Rao, S. A., and T. Yamagata, 2004: Abrupt termination of Indian Ocean dipole events in response to intraseasonal disturbances. *Geophys. Res. Lett.,* **31,** L19306, doi:10.1029/2004GL020842.

——, S. Masson, J. J. Luo, S. K. Behera, and T. Yamagata, 2007: Termination of Indian Ocean dipole events in a coupled general circulation model. *J. Climate,* **20,** 3018–3035.

——, J.-J. Luo, S. K. Behera, and T. Yamagata, 2008: Generation and termination of Indian Ocean dipole events in 2003, 2006 and 2007. *Climate Dyn.,* **33,** 751–767, doi:10.1007/s00382-008-0498-z.

Reid, J. S., and Coauthors, 2012: Multi-scale meteorological conceptual analysis of observed active fire hotspot activity and smoke optical depth in the Maritime Continent. *Atmos. Chem. Phys.,* **12,** 2117–2147, doi:10.5194/acp-12-2117-2012.

Resplandy, L., J. Vialard, M. Lévy, O. Aumont, and Y. Dandonneau, 2009: Seasonal and intraseasonal biogeochemical variability in the thermocline ridge of the southern tropical Indian Ocean. *J. Geophys. Res.,* **114,** C07024, doi:10.1029/2008JC005246.

Roundy, P. E., 2012: Tropical-extratropical interactions. *Intraseasonal Variability of the Atmosphere–Ocean Climate System,* 2nd ed. W. K.-M. Lau and D. E. Waliser, Eds., Springer, 497–512.

——, K. MacRitchie, J. Asuma, and T. Melino, 2010: Modulation of the global atmospheric circulation by combined activity in the Madden–Julian oscillation and the El Niño–Southern Oscillation during boreal winter. *J. Climate,* **23,** 4045–4059.

Saji, N. H., B. N. Goswami, P. N. Vinayachandran, and T. Yamagata, 1999: A dipole mode in the tropical Indian Ocean. *Nature,* **401,** 360–363.

Sassi, F., M. Salby, H. C. Pumphrey, and W. G. Read, 2002: Influence of the Madden-Julian oscillation on upper tropospheric humidity. *J. Geophys. Res.,* **107,** 4681, doi:10.1029/2001JD001331.

Schott, F., and J. P. McCreary, 2001: The monsoon circulation of the Indian Ocean. *Prog. Oceanogr.,* **51,** 1–123.

Schwartz, M. J., D. E. Waliser, B. Tian, D. L. Wu, J. H. Jiang, and W. G. Read, 2008: Characterization of MJO-related upper tropospheric hydrological processes using MLS. *Geophys. Res. Lett.,* **35,** L08812, doi:10.1029/2008GL033675.

Seiki, A., and Y. N. Takayabu, 2007a: Westerly wind bursts and their relationship with intraseasonal variations and ENSO. Part I: Statistics. *Mon. Wea. Rev.,* **135,** 3325–3345.

——, and ——, 2007b: Westerly wind bursts and their relationship with intraseasonal variations and ENSO. Part II: Energetics over the western and central Pacific. *Mon. Wea. Rev.,* **135,** 3346–3361.

——, ——, T. Yasuda, N. Sato, C. Takahashi, K. Yoneyama, and R. Shirooka, 2011: Westerly wind bursts and their relationship with ENSO in CMIP3 models. *J. Geophys. Res.,* **116,** D03303, doi:10.1029/2010JD015039.

Senan, R., D. Sengupta, and B. N. Goswami, 2003: Intraseasonal "monsoon jets" in the equatorial Indian Ocean. *Geophys. Res. Lett.,* **30,** 1750, doi:10.1029/2003GL017583.

Sengupta, D., R. Senan, B. N. Goswami, and J. Vialard, 2007: Intraseasonal variability of equatorial Indian Ocean zonal currents. *J. Climate,* **20,** 3036–3055.

Shapiro, M., and Coauthors, 2010: An Earth-System prediction initiative for the twenty-first century. *Bull. Amer. Meteor. Soc.,* **91,** 1377–1388.

Shi, L., O. Alves, H. H. Hendon, G. Wang, and D. Anderson, 2009: The role of stochastic forcing in ensemble forecasts of the 1997/98 El Nino. *J. Climate,* **22,** 2526–2540.

Shibagaki, Y., and Coauthors, 2006: Multi-scale convective systems associated with intraseasonal variation over the Indonesian maritime continent. *Mon. Wea. Rev.,* **134,** 1682–1696.

Slade, S. A., and E. D. Maloney, 2013: An intraseasonal prediction model of Atlantic and east Pacific tropical cyclone genesis. *Mon. Wea. Rev.,* **141,** 1925–1942.

Son, S.-W., and S. Lee, 2007: Intraseasonal variability of the zonal-mean extratropical tropopause height. *J. Atmos. Sci.,* **64,** 2695–2708.

Souza, E. B., and T. Ambrizzi, 2006: Modulation of the intraseasonal rainfall over tropical Brazil by the Madden–Julian oscillation. *Int. J. Climatol.,* **26,** 1759–1776.

Sperber, K. R., J. M. Slingo, and P. M. Inness, 2012: Modeling intraseasonal variability. *Intraseasonal Variability of the Atmosphere–Ocean Climate System,* 2nd ed. W. K.-M. Lau and D. E. Waliser, Eds., Springer, 399–432.

Stan, C., M. Khairoutdinov, C. A. DeMott, V. Krishnamurthy, D. M. Straus, D. A. Randall, J. L. Kinter III, and J. Shukla, 2010: An ocean-atmosphere climate simulation with an embedded cloud resolving model. *Geophys. Res. Lett.,* **37,** L01702, doi:10.1029/2009GL040822.

Tangang, F. T., L. Juneng, E. Salimun, P. N. Vinayachandran, Y. K. Seng, C. J. C. Reason, S. K. Behera, and T. Yasunari, 2008: On the roles of the northeast cold surge, the Borneo vortex, the Madden-Julian oscillation, and the Indian Ocean dipole during the extreme 2006/2007 flood in southern peninsular Malaysia. *Geophys. Res. Lett.,* **35,** L14S07, doi:10.1029/2008GL033429.

Thompson, D. B., and P. E. Rounday, 2013: The relationship between the Madden–Julian oscillation and U.S. violent tornado outbreaks in the spring. *Mon. Wea. Rev.,* **141,** 2087–2095.

Thompson, D. W. J., and J. M. Wallace, 2000: Annular modes in the extratropical circulation. Part I: Month-to-month variability. *J. Climate,* **13,** 1000–1016.

——, and ——, 2001: Regional climate impacts of the Northern Hemisphere annular mode. *Science,* **293,** 85–89.

Tian, B., and W. E. Waliser, 2012: Chemical and biological impacts. *Intraseasonal Variability of the Atmosphere–Ocean Climate System,* 2nd ed. W. K.-M. Lau and D. E. Waliser, Eds., Springer, 569–586.

——, C. O. Ao, D. E. Waliser, E. J. Fetzer, A. J. Mannucci, and J. Teixeira, 2012: Intraseasonal temperature variability in the upper troposphere and lower stratosphere from the GPS radio occultation measurements. *J. Geophys. Res.,* **117,** D15110, doi:10.1029/2012JD017715.

Vecchi, G. A., and N. A. Bond, 2004: The Madden-Julian oscillation (MJO) and northern high latitude wintertime surface air temperatures. *Geophys. Res. Lett.,* **31,** L04104, doi:10.1029/2003GL018645.

Ventrice, M. J., C. D. Thorncroft, and P. E. Roundy, 2011: The Madden–Julian oscillation's influence on African easterly waves and downstream tropical cyclogenesis. *Mon. Wea. Rev.,* **139,** 2704–2722.

Virts, K. S., and J. M. Wallace, 2010: Annual, interannual, and intraseasonal variability of tropical tropopause transition layer cirrus. *J. Atmos. Sci.,* **67,** 3097–3112.

——, J. A. Thornton, J. M. Wallace, M. L. Hutchins, R. H. Holzworth, and A. R. Jacobson, 2011: Daily and intraseasonal relationships between lightning and

NO_2 over the Maritime Continent. *Geophys. Res. Lett.,* **38,** L19803, doi:10.1029/2011GL048578.
Vitart, F., 2009: Impact of the Madden–Julian oscillation on tropical storms and risk of landfall in the ECMWF forecast system. *Geophys. Res. Lett.,* **36,** L15802, doi:10.1029/2009GL039089.
——, and F. Molteni, 2010: Simulation of the Madden–Julian oscillation and its teleconnections in the ECMWF forecast system. *Quart. J. Roy. Meteor. Soc.,* **136,** 842–855.
——, A. Leroy, and M. C. Wheeler, 2010: A comparison of dynamical and statistical predictions of weekly tropical cyclone activity in the Southern Hemisphere. *Mon. Wea. Rev.,* **138,** 3671–3682.
Waliser, D. E., 2012: Predictability and forecasting. *Intraseasonal Variability of the Atmosphere–Ocean Climate System,* 2nd ed. W. K.-M. Lau and D. E. Waliser, Eds., Springer, 433–476.
——, K. M. Lau, W. Stern, and C. Jones, 2003a: Potential predictability of the Madden–Julian oscillation. *Bull. Amer. Meteor. Soc.,* **84,** 33–50.
——, R. Murtugudde, and L. E. Lucas, 2003b: Indo-Pacific Ocean response to atmospheric intraseasonal variability: 1. Austral summer and the Madden–Julian Oscillation. *J. Geophys. Res.,* **108,** 3160, doi:10.1029/2002JC001620.
——, and Coauthors, 2006: The Experimental MJO Prediction Project. *Bull. Amer. Meteor. Soc.,* **87,** 425–431.
——, B. Tian, X. Xie, W. T. Liu, M. J. Schwartz, and E. J. Fetzer, 2009: How well can satellite data characterize the water cycle of the Madden-Julian Oscillation? *Geophys. Res. Lett.,* **36,** L21803, doi:10.1029/2009GL040005.
Wallace, J. M., and D. S. Gutzler, 1981: Teleconnections in the geopotential height field during the Northern Hemisphere winter. *Mon. Wea. Rev.,* **109,** 784–812.
Wang, B., 2012: Theories. *Intraseasonal Variability of the Atmosphere–Ocean Climate System*, 2nd ed. W. K.-M. Lau and D. E. Waliser, Eds., Springer, 335–398.
Wang, C.-C., and G. Magnusdottir, 2006: The ITCZ in the central and eastern Pacific on synoptic time scales. *Mon. Wea. Rev.,* **134,** 1405–1421.
Webster, P. J., A. W. Moore, J. P. Loschnigg, and R. R. Leben, 1999: Coupled ocean-atmosphere dynamics in the Indian Ocean during 1997–98. *Nature,* **401,** 356–360.
Wheeler, M. C., and H. H. Hendon, 2004: An all-season real-time multivariate MJO index: Development of an index for monitoring and prediction. *Mon. Wea. Rev.,* **132,** 1917–1932.
——, and J. L. McBride, 2012: Australian monsoon. *Intraseasonal Variability of the Atmosphere–Ocean Climate System,* 2nd ed. W. K.-M. Lau and D. E. Waliser, Eds., Springer, 147–198.
——, H. H. Hendon, S. Cleland, H. Meinke, and A. Donald, 2009: Impacts of the MJO on Australian rainfall and circulation. *J. Climate,* **22,** 1482–1497.
Wong, S., and A. E. Dessler, 2007: Regulation of H_2O and CO in tropical tropopause layer by the Madden–Julian oscillation. *J. Geophys. Res.,* **112,** D14305, doi:10.1029/2006JD007940.
Wu, X., L. Deng, X. Song, G. Vettoretti, W. R. Peltier, and G. J. Zhang, 2007: Impact of a modified convective scheme on the Madden-Julian oscillation and El Niño–Southern Oscillation in a coupled climate model. *Geophys. Res. Lett.,* **34,** *L16823,* doi:10.1029/2007GL030637.
Wyrtki, K., 1973: An equatorial jet in the Indian Ocean. *Science,* **181,** 262–264.
——, 1987: Indonesian throughflow and the associated pressure gradient. *J. Geophys. Res.,* **92** (C12), 12 941–12 946.
Yamakawa, S., and R. Suppiah, 2009: Extreme climatic events in recent years and their links to large-scale atmospheric circulation features. *Global Environ. Res.,* **13,** 69–78.
Yoneyama, K., C. Zhang, and C. Long, 2013: Tracking pulses of the Madden–Julian oscillation. *Bull. Amer. Meteor. Soc.,* **94,** 1871–1891.
Yoo, C., S. Feldstein, and S. Lee, 2011: The impact of the Madden-Julian oscillation trend on the Arctic amplification of surface air temperature during the 1979–2008 boreal winter. *Geophys. Res. Lett.,* **38,** L24804, doi:10.1029/2011GL049881.
——, S. Lee, and S. Feldstein, 2012: Mechanisms of arctic surface air temperature change in response to the Madden–Julian oscillation. *J. Climate,* **25,** 5777–5790.
Zavala-Garay, J., C. Zhang, A. M. Moore, A. Wittenberg, M. Harrison, A. Rosati, A. T. Weaver, and J. Vialard, 2008: Sensitivity of hybrid ENSO models to uncoupled atmospheric variability. *J. Climate,* **21,** 3704–3721.
Zhan, Z., J. Li, and A. Gettelman, 2006: Intraseasonal variations of upper tropospheric water vapor in Asian monsoon region. *Atmos. Chem. Phys. Discuss.,* **6,** 8069–8095.
Zhang, C., 2005: Madden-Julian Oscillation. *Rev. Geophys.,* **43,** RG2003, doi:10.1029/2004RG000158.
——, 2012: Vertical structure from recent observations. *Intraseasonal Variability of the Atmosphere–Ocean Climate System,* 2nd ed. W. K.-M. Lau and D. E. Waliser, Eds., Springer, 537–548.
——, and J. Gottschalck, 2002: SST anomalies of ENSO and the Madden–Julian oscillation in the equatorial Pacific. *J. Climate,* **15,** 2429–2445.
Zhang, L., B. Wang, and Q. Zeng, 2009: Impact of the Madden–Julian oscillation on summer rainfall in southeast China. *J. Climate,* **22,** 201–216.

Zhou, L., and R. Murtugudde, 2010: Influences of Madden–Julian oscillations on the eastern Indian Ocean and the maritime continent. *Dyn. Atmos. Oceans,* **2,** 257–274, doi:10.1016/j.dynatmoce.2009.12.003.

——, ——, and M. Jochum, 2008: Dynamics of the Intraseasonal oscillations in the Indian Ocean South Equatorial Current. *J. Phys. Oceanogr.,* **38,** 121–132.

Zhou, S., M. L'Heureux, S. Weaver, and A. Kumar, 2012: A composite study of the MJO influence on the surface air temperature and precipitation over the continental United States. *Climate Dyn.,* **38,** 1459–1471, doi:10.1007/s00382-011-1001-9.

Zhou, X., and J. R. Holton, 2002: Intraseasonal variations of tropical cold-point tropopause temperatures. *J. Climate,* **15,** 1460–1473.

Zhu, C., T. Nakazawa, J. Li, and L. Chen, 2003: The 30–60 day intraseasonal oscillation over the western North Pacific Ocean and its impacts on summer flooding in China during 1998. *Geophys. Res. Lett.,* **30,** 1952, doi:10.1029/2003GL017817.